MICROCOPY RESOLUTION TEST CHART

AD

AMMRC TR 79-29

STRESS ANALYSIS AND STRENGTH CHARACTERIZATION OF THICK
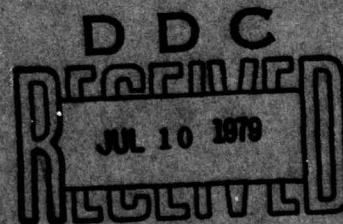COMPOSITE LAMINATES

MAY 1979

WASHINGTON UNIVERSITY
MATERIALS RESEARCH LABORATORY
ST. LOUIS, MO 63130

FINAL REPORT   CONTRACT NUMBER DAAG46-75-C-0096

Approved for public release; distribution unlimited.

D D C
RECEIVED
JUL 10 1979
B

Prepared for

ARMY MATERIALS AND MECHANICS RESEARCH CENTER
Watertown, Massachusetts 02172

79 07 09 208

REPORT DOCUMENTATION PAGE		READ INSTRUCTIONS BEFORE COMPLETING FORM
1. REPORT NUMBER AMMRC TR-79-29	2. GOVT ACCESSION NO.	3. RECIPIENT'S CATALOG NUMBER
4. TITLE (and Subtitle) Stress Analysis and Strength Characterization of Thick Composite Laminates.		5. TYPE OF REPORT & PERIOD COVERED Final Report
		6. PERFORMING ORG. REPORT NUMBER
7. AUTHOR(s) Edward M. Wu, King Him Lo. Richard M. Christensen		8. CONTRACT OR GRANT NUMBER(s) DAAG46-75-C-0096
9. PERFORMING ORGANIZATION NAME AND ADDRESS Army Materials & Mechanics Research Center Watertown, Massachusetts 02172		10. PROGRAM ELEMENT, PROJECT, TASK AREA & WORK UNIT NUMBERS D/A Project: 8X363304D215 AMCMS Code: 633304.21500.03 Agency Accession:
11. CONTROLLING OFFICE NAME AND ADDRESS Army Materials and Mechanics Research Center Watertown, Massachusetts 02172		12. REPORT DATE May 1979
		13. NUMBER OF PAGES 12
14. MONITORING AGENCY NAME & ADDRESS(if different from Controlling Office) 8X363304D215		15. SECURITY CLASS. (of this report) Unclassified
		15a. DECLASSIFICATION/DOWNGRADING SCHEDULE

16. DISTRIBUTION STATEMENT (of this Report)

Approved for public release; distribution unlimited.

17. DISTRIBUTION STATEMENT (of the abstract entered in Block 20, if different from Report)

DDC
RECEIVED
JUL 10 1979
B

18. SUPPLEMENTARY NOTES

19. KEY WORDS (Continue on reverse side if necessary and identify by block number)

Composites	Mechanical tests	Stresses
Lamina	Elasticity	
Plate theory	Fracture strength	

20. ABSTRACT (Continue on reverse side if necessary and identify by block number)

See Block No. 20.

DD FORM 1473 EDITION OF 1 NOV 65 IS OBSOLETE
1 JAN 73

408 186

<u>Block No. 20</u>

ABSTRACT

This final report covers the theoretical development of and experimental results for the stress analysis and strength characterization of thick composite laminates. Thick composite laminates (consisting of 38 plies or more) are being evaluated for use in future high performance anti-ballistic missiles and other aerospace applications. The theoretical development includes the derivation of a high-order theory of plate deformation which accounts for the effects of transverse shear deformation, transverse normal strain, and a non-linear distribution of the in-plane displacements with respect to the thickness coordinates. The theory is developed for both homogeneous and laminated plates and is presented respectively in Chapters 1 and 2. Chapter 3 presents further examination of this high-order plate theory via stress solutions which have been carried out to assess its accuracy. This theory, in effect, enables close estimation of three-dimensional stress components from essentially two-dimensional analysis.

The effects of the three-dimensional state of stress on the strength of a thick laminates are analysed with a 3-D failure criterion. In Chapter 4, the tensor polynomial method is extended with full account given to three-dimensional stress state effects and is presented together with experiment and evaluation of the coefficients. The combined theoretical development of thick-plate analysis and three-dimensional failure criterion is expected to improve confidence and full utilization of composites in applications where the thickness of the laminates prevents them from being adequately treated by current thin-plate formulations.

* is reported

FOREWARD

This final report is prepared by Washington University for the Army Materials and Mechanics Research Center AMMRC, Watertown, Massachusetts under contract DAAG-46-75-C-0096. This contract is part of an advanced Composite Structures Program under the direction of Mr. John Dignam, ABM Materials Hardening Program Manager and monitored by Dr. S. C. Chou. Specimens from which experimental data were collected were supplied by the Government.

TABLE OF CONTENTS

SUMMARY

This final report covers the theoretical development of and experimental results for the stress analysis and strength characterization of thick composite laminates. Thick composite laminates (consisting of 38 plies or more) are being evaluated for use in future high performance anti-ballistic missiles and other aerospace applications. The theoretical development includes the derivation of a high-order theory of plate deformation which accounts for the effects of transverse shear deformation, transverse normal strain, and a non-linear distribution of the in-plane displacements with respect to the thickness coordinates. The theory is developed for both homogeneous and laminated plates and is presented respectively in Chapters 1 and 2. Chapter 3 presents further examination of this high-order plate theory via stress solutions which have been carried out to assess its accuracy. This theory, in effect, enables close estimation of three-dimensional stress components from essentially two-dimensional analysis.

The effects of the three-dimensional state of stress on the strength of a thick laminates are analysed with a 3-D failure criterion. In Chapter 4, the tensor polynomial method is extended with full account given to three-dimensional stress state effects and is presented together with experiment and evaluation of the coefficients. The combined theoretical development of thick-plate analysis and three-dimensional failure criterion is expected to improve confidence and full utilization of composites in applications

1

where the thickness of the laminates prevents them from being adequately
treated by current thin-plate formulations.

INTRODUCTION

In many structural applications, special characterization methods
are needed to model very thick, laminated composites. These thick
composites are currently being evaluated for future high performance
antiballistic missiles and other aerospace applications. A rational
characterization must include 1) extending current two-dimensional
laminated-plate theory to reflect the three-dimensional characteristic
of these thick plates for the purpose of accurately estimating
deflection and the three-dimensional state of stress, 2) establishing
failure criterion to assess the effect of the three-dimensional state
of stress and hence of the strength of a thick laminate. In light of
these requirements, a high-order plate deformation theory is derived
to remove the restriction of the plane-section-remains-plane
hypothesis in conventional laminated plate theory by allowing a
plane section to assume third-order displacement modes. This theory
is fully developed for homogeneous and laminated plates and is
presented, together with stress solutions, in chapters 1, 2 and 3.
In order to present the theory in complete and concise form the
theories and stress solution are presented in the format of self-
contained chapters. Finally the effects of a three-dimensional state
of stress on the strength of the thick laminates are assessed with
a three-dimensional tensor polynomial failure criterion in chapter 4.
These four chapters together provide the necessary tools for the
stress analysis and strength characterization of thick laminates
composites. These tools should enhance a more complete and confident
utilization of composites in the form of thick laminates.

3

Chapter 1

A HIGH ORDER THEORY OF PLATE DEFORMATION

Homogeneous Plates

K. H. Lo, R. M. Christensen, and E. M. Wu

4

ABSTRACT

A theory of plate deformation is derived which accounts for the effects of transverse shear deformation, transverse normal strain, and a nonlinear distribution of the in-plane displacements with respect to the thickness coordinate. The theory is compared with lower order plate theories through application to a particular problem involving a plate acted upon by a sinusoidal surface pressure. Comparison is also made with the exact elasticity solution of this problem. It is found that when the ratio of the characteristic length of the load pattern to the plate thickness is of the order of unity, lower order theories are inadequate and the present high order theory is required to give meaningful results. The present work treats homogeneous plates while Chapter II involves laminated plates.

INTRODUCTION

The development and application of classical plate theory is one of the achievements of modern engineering. It is continuously being applied to new problems to gain new and needed design information. Despite its successes, however, the inherent limitations of the classical theory necessitate the development of more refined and higher order theories of plate behavior. More sophisticated models of plate behavior find application to problems where classical plate theory is simply inadequate to describe the behavior. Such examples concern plate with cutouts, contact problems involving plates, and laminated plates. The present work concerns the derivation and evaluation of a particular high order theory of plate behavior.

Before describing the present theory, it is necessary to briefly
review the recent developments in the generalization of classical
plate theory. Reissner [1,2] was the first to provide a consistent
theory which incorporates the effect of shear deformation. The derivation
given by Reissner resulting in displacements of the form

$$u = u^\circ + z\psi_x$$
$$v = v^\circ + z\psi_y \qquad\qquad (1)$$
$$w = w^\circ$$

where z is the coordinate normal to the middle plane, and u°, v°,
ψ_x, ψ_y, and w° have a dependence upon the in-plane coordinates x and y,
and ψ_x, ψ_y, and w° are actually weighted averages. The basic
assumption used by Reissner involved consistent forms for the stress
distributions across the thickness. A special variational theorem was
used to determine both the equations of equilibrium in terms of
resultants and the stress-strain relations in the form involving
resultants and the functions in (1). At the same level of approximation,
Mindlin [3] employed kinematic assumptions of the form of (1), and
without introducing corresponding stress distribution assumptions,
obtained the governing equations from a direct method. In Mindlin's
derivation it was necessary to introduce a correction factor into
the shear stress resultants to account for the fact that relations (1)
predict a uniform shear stress through the thickness of the plate,
which is incorrect and in general would violate surface conditions.
The correction factor was evaluated by comparison with an exact
elasticity solution. It is useful to observe that the form (1) applies

to both the classical theory of plate bending as well as to the theories of Reissner and Mindlin which include the effect of transverse shear deformation. Thus, considering the terms in (1) as the first terms in a power series expansion in z, it is seen that the classical theory and the shear deformation theory are of the same order of approximation. The classical theory is merely a special case of the shear deformation theory, wherein the shear modulus in terms associated with the transverse shear deformation is taken to be very large, such that transverse shear deformation can be neglected.

There have been several theories proposed which are of higher order than those of Reissner and Mindlin. Typical efforts along these lines will be mentioned here. The next higher order theory from that embodied in (1) involves displacement forms of type

$$u = u^\circ + z\psi_x$$
$$v = v^\circ + z\psi_y \tag{2}$$
$$w = w^\circ + z\psi_z + z^2\zeta_z$$

which invludes the effect of transverse normal strain. Displacement assumptions of the form of (2) along with corresponding stress distribution assumptions have been used by Naghdi [4] to derive a general theory of shells, and by Essenburg [5] to derive the corresponding one-dimensional plate theory. In the context of contact problems, Essenburg [5] demonstrated the utility and advantages of the theory based upon (2) over lower order theories. Whitney and Sun [6] also utilized assumptions of the level of (2) to develop a theory of lamianted cylindrical shells. However, there is an inconsistency in

7

their approach. They used a shear correction factor of the same type as that employed by Mindlin in deriving stress resultants. Whereas a factor of this type was appropriate to Mindlin's derivation since it assumed uniform shear stresses across the thickness, the same type of correction factor is not appropriate for use with the displacements of the form of (2). This is because non-uniform shear stresses are implied by (2) along with consequent satisfaction of top and bottom boundary conditions of shear tractions; thus the rationale for a correction factor is obviated.

The next higher level theory is based upon the assumed displacement forms

$$u = u^\circ + z\psi_x + z^2\zeta_x$$
$$v = v^\circ + z\psi_y + z^2\zeta_y \qquad (3)$$
$$w = w^\circ + z\psi_z + z^2\zeta_z$$

A theory derived from (3) has been given by Nelson and Lorch [7] for application to laminates. This theory however has the same defect in application as that mentioned above in connection with Ref. [6]; namely, a shear correction factor was employed when in fact it is inconsistent with the level of approximation in (3). Hildebrand, Reissner and Thomas [8] briefly examined a theory of the level of (3) and concluded that the inclusion of the quadratic terms in the in-plane displacements does not provide a significant advantage over the lower level theory.

Reissner [9] has presented a theory which to a consistent degree of approximation gives

8

$$u = z\psi_x + z^3\phi_x$$
$$v = z\psi_y + z^3\phi_y \qquad (4)$$
$$w = w^\circ + z^2\zeta_z$$

where the last relation in (4) follows by combining relations (9) and
(11) of Ref. [9]. Reissner has shown that the plate theory corresponding
to (4) gives very accurate results compared with the elasticity solution
for the bending of a plate with a circular hole. It should be noted
that the theory based upon (4) represents the lowest order correction
for out-of-plane deformation effects to the classical theory embodied
in the first terms in (4). Though these results obtained by Reissner
are impressive, a theory based upon (4) neglects the contribution of
in-plane modes of deformation; only out-of-plane effects are considered.
Such in-plane effects may be of importance in certain plate problems,
and this effect will be investigated herein.

The theory to be presented here is appropriate to the following
displacement forms:

$$u = u^\circ + z\psi_x + z^2\zeta_x + z^3\phi_x$$
$$v = v^\circ + z\psi_y + z^2\zeta_y + z^3\phi_y \qquad (5)$$
$$w = w^\circ + z\psi_z + z^2\zeta_z$$

which is of the same level as the Reissner theory corresponding to
(4) but includes both in-plane and out-of-plane modes of deformation.
The theory of plate behavior based upon (5) will be derived by
application of the principle of stationary potential energy. The
accuracy of this theory will be assessed by direct comparison with an
exact solution from the theory of elasticity.

9

Before turning to the derivation, it is pertinent to outline the motivation for the present work. The primary intended application for the present high order plate theory is in the field of laminates. It is well known that laminated plate behavior provides a particularly critical test of the Bernoulli hypothesis concerning plane sections remaining plane. The mismatch in properties causes deviations from the lowest order terms in displacement forms (4). However, to place the present work in its proper context, it is useful to derive it first in the form directly suitable for application to homogeneous plates. Accordingly, the present paper, Chapter I is concerned with homogeneous plate behavior while Chapter II, following, is concerned with the application to laminates. The present work thus affords the opportunity to assess the importance of the full form of displacements (5) compared with the partial form (4) for certain types of problems. This same question will be further explored in the context of laminates in Chapter II.

Finally, it should be mentioned that a theory of the level of (5) certainly is of a rather complicated form, and the question arises whether there is a practical need for such a theory. It is a question of the degree of accuracy required. For problems which involve rapidly fluctuating loads with a characteristic length of the order of the thickness, the results presented herein show that a theory of the degree of sophistication of (5) is required to give meaningful results. Also, it should be recognized that the theory to be developed here is amenable to numerical integration with respect to the planar x,y coordinates.

10

THEORY

Plate theories can be developed by expanding the displacements in power series of the coordinate normal to the middle plane. In principle, theories developed by this means can be made as accurate as desired simply by including a sufficient number of terms. In practice, however, a point of diminishing returns is reached whereby the complexity of the resulting forms becomes too great. Here, we seek the minimum number of terms which include the effects of transverse shear deformation, transverse normal strain, and warpage of the cross section. Thus the displacements are taken in the form of (5).

The principle of stationary potential energy is used to derive the governing equilibrium equations. It is found that

$$
\begin{aligned}
&N_{x,x} + N_{xy,y} + q_x = 0 \\
&N_{y,y} + N_{xy,x} + q_y = 0 \\
&Q_{x,x} + Q_{y,y} + q = 0 \\
&M_{x,x} + M_{xy,y} - Q_x + m_x = 0 \\
&M_{y,y} + M_{xy,x} - Q_y + m_y = 0 \\
&R_{x,x} + R_{y,y} - N_z + m = 0 \\
&P_{x,x} + P_{xy,y} - 2R_x + n_x = 0 \\
&P_{y,y} + P_{xy,x} - 2R_y + n_y = 0 \\
&S_{x,x} + S_{y,y} - 2M_z + n = 0 \\
&\overline{M}_{x,x} + \overline{M}_{xy,y} - 3S_x + \ell_x = 0 \\
&\overline{M}_{y,y} + \overline{M}_{xy,x} - 3S_y + \ell_y = 0
\end{aligned}
\tag{6}
$$

11

where the stress resultants are defined by

$$
\begin{bmatrix}
N_x & N_y & N_z & N_{xy} & Q_x & Q_y \\
M_x & M_y & M_z & M_{xy} & R_x & R_y
\end{bmatrix}
= \int_{-h/2}^{h/2}
\begin{Bmatrix} 1 \\ z \end{Bmatrix}
[\sigma_x \ \sigma_y \ \sigma_z \ \tau_{xy} \ \tau_{xz} \ \tau_{yz}] dz \quad (7)
$$

$$
\begin{bmatrix}
P_x & P_y & P_{xy} \\
\overline{M}_x & \overline{M}_y & \overline{M}_{xy}
\end{bmatrix}
= \int_{-h/2}^{h/2}
\begin{Bmatrix} z^2 \\ z^3 \end{Bmatrix}
(\sigma_x \ \sigma_y \ \tau_{xy}) \, dz \quad (8)
$$

and

$$
[S_x \ S_y] = \int_{-h/2}^{h/2} z^2 \, (\tau_{xz} \ \tau_{yz}) \, dz \quad (9)
$$

with

$$
\begin{aligned}
(q_x \ \ n_x) &= [\tau_{xz}(h/2)-\tau_{xz}(-h/2)] \ [1 \ \ h^2/4] \\
(q_y \ \ n_y) &= [\tau_{yz}(h/2)-\tau_{yz}(-h/2)] \ [1 \ \ h^2/4] \\
(m_x \ \ \ell_x) &= [\tau_{xz}(h/2) + \tau_{xz}(-h/2)] \ [h/2 \ \ h^3/8] \\
(m_y \ \ \ell_y) &= [\tau_{yz}(h/2) + \tau_{yz}(-h/2)] \ [h/2 \ \ h^3/8] \\
(q \ \ n) &= [\sigma_z(h/2)- \sigma_z(-h/2) \ [1 \ \ h^2/4] \\
m &= \frac{h}{2} \ [\sigma_z(h/2) + \sigma_z(-h/2)]
\end{aligned} \quad (10)
$$

The resultants in terms of the displacement functions are given by

$$
N_x = (\lambda+2\mu)hu^\circ,_x + \lambda hv^\circ,_y + \lambda h\psi_z + \frac{h^3}{12} [(\lambda+2\mu) \zeta_{x,x} + \lambda \zeta_{y,y}]
$$

$$
N_y = \lambda hu^\circ,_x + (\lambda+2\mu)hv^\circ,_y + \lambda h\psi_z + \frac{h^3}{12} [\lambda \zeta_{x,x} + (\lambda+ 2\mu)\zeta_{y,y}]
$$

$$
N_z = \lambda hu^\circ,_x + \lambda hv^\circ,_y + (\lambda+2\mu)h\psi_z + \frac{h^3}{12} [\lambda\zeta_{x,x}+\lambda\zeta_{y,y}] \quad (11)
$$

$$
N_{xy} = \mu h[u^\circ,_y + v^\circ,_x] + \frac{\mu h^3}{12} [\zeta_{x,y} + \zeta_{y,x}]
$$

12

$$M_x = \frac{h^3}{12} \left[(\lambda+2\mu)\psi_{x,x} + \lambda\psi_{y,y} + 2\lambda\zeta_z \right)$$

$$+ \frac{h^5}{80} \left[(\lambda+2\mu)\phi_{x,x} + \lambda\phi_{y,y} \right]$$

$$M_y = \frac{h^3}{12} \left[\lambda\psi_{x,x} + (\lambda+2\mu)\psi_{y,y} + 2\lambda\zeta_z \right]$$

$$+ \frac{h^5}{80} \left[\lambda\phi_{x,x} + (\lambda+2\mu)\phi_{y,y} \right] \qquad (12)$$

$$M_z = \frac{h^3}{12} \left[\lambda\psi_{x,x} + \lambda\psi_{y,y} + 2(\lambda+2\mu)\zeta_z \right]$$

$$+ \frac{h^5}{80} \left[\lambda\phi_{x,x} + \lambda\phi_{y,y} \right]$$

$$M_{xy} = \frac{\mu h^3}{12} \left[\psi_{x,y} + \psi_{y,x} \right] + \frac{\mu h^5}{80} \left[\phi_{x,y} + \phi_{y,x} \right]$$

$$P_x = \frac{h^3}{12} \left[(\lambda+2\mu)u^\circ_{,x} + \lambda v^\circ_{,y} + \lambda\psi_z \right]$$

$$+ \frac{h^5}{80} \left[(\lambda+2\mu)\zeta_{x,x} + \lambda\zeta_{y,y} \right]$$

$$P_y = \frac{h^3}{12} \left[\lambda u^\circ_{,x} + (\lambda+2\mu)v^\circ_{,y} + \lambda\psi_z \right] \qquad (13)$$

$$+ \frac{h^5}{80} \left[\lambda\zeta_{x,x} + (\lambda+2\mu)\zeta_{y,y} \right]$$

$$P_{xy} = \frac{\mu h^3}{12} \left[u^\circ_{,y} + v^\circ_{,x} \right] + \frac{\mu h^5}{80} \left[\zeta_{x,y} + \zeta_{y,x} \right]$$

$$\overline{M}_x = \frac{h^5}{80} \left[(\lambda+2\mu)\psi_{x,x} + \lambda\psi_{y,y} + 2\lambda\zeta_z \right]$$

$$+ \frac{h^7}{448} \left[(\lambda+2\mu)\phi_{x,x} + \lambda\phi_{y,y} \right]$$

$$\overline{M}_y = \frac{h^5}{80} \left[\lambda\psi_{x,x} + (\lambda+2\mu)\psi_{y,y} + 2\lambda\zeta_z \right] \qquad (14)$$

$$+ \frac{h^7}{448} \left[\lambda\phi_{x,x} + (\lambda+2\mu)\phi_{y,y} \right]$$

$$\overline{M}_{xy} = \frac{\mu h^5}{80} \left[\psi_{x,y} + \psi_{y,x} \right] + \frac{\mu h^7}{448} \left[\phi_{x,y} + \phi_{y,x} \right]$$

$$Q_x = \mu h [\psi_x + \cdot w^\circ,_x] + \frac{\mu h^3}{12} \ [3\phi_x + \zeta_{z,x}]$$

$$Q_y = \mu h [\psi_y + w^\circ,_y] + \frac{\mu h^3}{12} \ [3\phi_y + \zeta_{z,y}] \tag{15}$$

$$R_x = \frac{\mu h^3}{12} \ [2\zeta_x + \psi_{z,x}]$$

$$R_y = \frac{\mu h^3}{12} \ [2\zeta_y + \psi_{z,y}] \tag{16}$$

·and

$$S_x = \frac{\mu h^3}{12} \ [\psi_x + w^\circ,_x] + \frac{\mu h^5}{80} \ [3\phi_x + \zeta_{z,x}]$$

$$S_y = \frac{\mu h^3}{12} \ [\psi_y + w^\circ,_y] + \frac{\mu h^5}{80} \ [3\phi_y + \zeta_{z,y}] \tag{17}$$

where λ and u are the Lamé constants.

Finally, the boundary conditions along the edge of the plate require that one member of each of the following eleven products must be presecribed:

$N_n \ u^\circ_n, \ N_{nt} \ u^\circ_t, \ M_n \ \psi_n$

$M_{nt} \ \psi_t, \ P_n \ \zeta_n, \ P_{nt} \ \zeta_t$

$\overline{M}_n \ \phi_n, \ \overline{M}_{nt} \ \phi_t, \ Q_n w^\circ$

$R_n \ \psi_z$ and $S_n \ \zeta_z$

where n and t are the directions normal and tangential to the edge of the plate.

14

When expressed in terms of displacements, relations (6) comprise a set of eleven coupled second order partial differential equations which govern the behavior of the present plate theory.

EVALUATION OF PLATE THEORIES

An approximate theory can be critically assessed in comparison with an exact result. Fortunately, there are exact solutions available from the theory of elasticity which are suitable for the present purposes. The solution of use here is that of the deformation of an infinite plate of thickness h subjected to a pressure on the top surface $z = h/2$ of the form

$$q = q_o \sin \frac{\pi x}{L} \tag{18}$$

with all other surface tractions vanishing identically. From equations (1) it follows that

$$q_x = q_y = m_x = m_y = n_x = n_y = \ell_x = \ell_y = 0 \tag{19}$$

with

$$m = \frac{h}{2} q_o \sin \frac{\pi x}{L}$$

$$n = \frac{h^2}{4} q_o \sin \frac{\pi x}{L} \tag{20}$$

The equations of equilibrium (6) take the following special forms for this problem

15

$$\mu h[\psi_{x,x} + w^\circ{}_{,xx}] + \frac{\mu h^3}{12}[3\phi_{x,x} + \zeta_{z,xx}] + q = 0$$

$$\frac{h^3}{12}[(\lambda+2\mu)\psi_{x,xx} + 2\lambda\zeta_{z,x}] + \frac{h^5}{80}[(\lambda+2\mu)\phi_{x,xx}]$$

$$-\mu h[\psi_x + w^\circ{}_{,x}] - \frac{\mu h^3}{12}[3\phi_x + \zeta_{z,x}] = 0$$

$$\frac{h^3}{12}[(\mu-2\lambda)\psi_{x,x} + \mu w^\circ{}_{,xx} - 4(\lambda+2\mu)\zeta_z]$$

$$+ \frac{h^5}{80}[(3\mu-2\lambda)\phi_{x,x} + \mu\zeta_{z,xx}] + n = 0$$

$$\frac{h^5}{80}[(\lambda+2\mu)\psi_{x,xx} + (2\lambda-3\mu)\zeta_{z,x} - 9\mu\phi_x]$$

$$+ \frac{h^5}{448}[(\lambda+2\mu)\phi_{x,xx}] - \frac{\mu h^3}{4}[\psi_x + w^\circ{}_{,x}] = 0$$

(21)

$$(\lambda+2\mu)hu^\circ{}_{,xx} + \lambda h\psi_{z,x} + (\lambda+2\mu)\frac{h^3}{12}\zeta_{x,xx} = 0$$

$$\frac{h^3}{12}[(2\mu-\lambda)\zeta_{x,x} + \mu\psi_{z,xx}] - \lambda hu^\circ{}_{,x} - (\lambda+2\mu)h\psi_z + m = 0$$

$$\frac{h^3}{12}[(\lambda+2\mu)u^\circ{}_{,xx} - 4\mu\zeta_x + (\lambda-2\mu)\psi_{z,x}]$$

$$+ \frac{h^5}{80}[(\lambda+2\mu)\zeta_{x,xx}] = 0$$

(22)

$$\mu h v^\circ{}_{,xx} + \frac{\mu h^3}{12}\zeta_{y,xx} = 0$$

$$\mu\frac{h^3}{12}v^\circ{}_{,xx} - 4\mu\frac{h^3}{12}\zeta_y + \frac{\mu h^5}{80}\zeta_{y,xx} = 0$$

(23)

16

and

$$\frac{\mu h^3}{12} \psi_{y,xx} + \frac{\mu h^5}{80} \phi_{y,xx} - \mu h \psi_y - \frac{\mu h^3}{4} \phi_y = 0$$

$$\frac{h^5}{80} [\mu \psi_{y,xx} - 9\mu\phi_y] + \frac{\mu h^7}{448} \phi_{y,xx} - \frac{\mu h^3}{4} \psi_y = 0$$

(24)

Note that the equations partially decouple such that the equation grouping in each of the above number sets are individually determinate.

Obviously, the solution for the generalized displacement functions involve terms proportional to sin πx/L and cos πx/L. Making the appropriate assumptions of this type, relations (21) - (24) can be solved analytically in closed form.

The completed solution can be used to evaluate the displacements and stress for comparison purposes. *The mid-plane displacement is* given by

$$w^\bullet = \frac{q_o}{D} \frac{L^4}{\pi^4} \cdot \left\{ 33600 \ (1-\nu)(1-2\nu) + [7200 - 16920\nu + 5520\nu^2] \ \pi^2 \left(\frac{h}{L}\right)^2 \right.$$

$$\left. + 140\nu(1-\nu)\pi^4 \left(\frac{h}{L}\right)^4 - (1-\nu)^2 \pi^6 \left(\frac{h}{L}\right)^6 \right\} \sin \frac{\pi x}{L}$$

(25)

$$\Big/ \left\{ 4(1-\nu) \left[8400 \ (1-2\nu) + 120 \ (1-\nu)\pi^2 \left(\frac{h}{L}\right)^2 + (1-\nu)^2 \pi^4 \left(\frac{h}{L}\right)^4 \right] \right\}$$

17

The solution for the stress component σ_x is given by

$$\sigma_x = q_o \left\{ \frac{15 (1-\nu)^2 \pi^2 (h/L)^2 [12 (z/h)^2 - 1]}{\left[720 (1-2\nu) + 24 (1-\nu)\pi^2 (h/L)^2 + (1-\nu)^2 \pi^4 (h/L)^4 \right]} \right.$$

$$+ \left[\frac{6}{\pi^2} \left(\frac{L}{h} \right)^2 \frac{z}{h} \quad [33600 (1-2\nu) - 120 (1-\nu)(10-7\nu) \frac{\pi^2 h^2}{L^2} \right.$$

$$- 80 (1-\nu)^2 \pi^4 \left(\frac{h}{L} \right)^4 \Bigg]$$

$$\left. + 12(1-\nu) \left(\frac{z}{h} \right)^3 [2800 (2-\nu) + 280 (1-\nu)\pi^2 \left(\frac{h}{L} \right)^2] \Bigg] \right\} \sin \frac{\pi x}{L}$$

$$\Bigg/ [16800 (1-2\nu) + 240 (1-\nu) \pi^2 \left(\frac{h}{L} \right)^2 + 2 (1-\nu)^2 \pi^4 \left(\frac{h}{L} \right)^4]$$

(26)

These results are to be compared with the exact solution, taken from Little [10]. Other lower order approximate theories also will be compared with the present results. First, the classical theory result is noted to be

$$w^\circ = \frac{q_o}{D} \frac{L^4}{\pi^4} \sin \left(\frac{\pi x}{L} \right)$$

(27)

The shear deformation Reissner plate theory produces the result

$$w^\bullet = \frac{q_o}{D} \frac{L^4}{\pi^4} \left[1 + \frac{\pi^2}{10} \cdot \frac{(2-\nu)}{(1-\nu)} \left(\frac{h}{L} \right)^2 \right] \sin \frac{\pi x}{L}$$

(28)

18

Essenburg's theory gives

$$w^\circ = \frac{q_o}{D} \frac{L^4}{\pi^4} \left[1 + \frac{\pi^2}{10} \cdot \frac{(2-\nu)}{(1-\nu)} \left(\frac{h}{L} \right)^2 + \frac{\pi^2}{10} \frac{\nu^2}{(1-\nu)} \left(\frac{h}{L} \right)^2 \right.$$
$$\left. + \frac{\nu\pi^2}{40} \left(\frac{h}{L} \right)^2 - \frac{3\pi^4}{1120} \left(\frac{h}{L} \right)^4 \right] \sin \frac{\pi x}{L} \tag{29}$$

Finally, for comparison, the present theory with $\zeta_x = \zeta_y = \phi_x = \phi_y = 0$ in (5) has been evaluated and will be referred to as the "Level (2) Theory", consistent with equations (2). This solution is

$$w^\circ = \frac{q_o}{D} \frac{L^4}{\pi^4} \left[1 + \frac{20\pi^2}{(1-\nu)\,[120 + (1-\nu)\pi^2\,(h/L)^2]} \left(\frac{h}{L} \right)^2 \right.$$
$$- \frac{1}{4(1-\nu)\,[120 + (1-\nu)\pi^2\,(h/L)^2]} \left[4\nu^2\pi^2 \left(\frac{h}{L} \right)^2 + 20\nu\pi^2 \left(\frac{h}{L} \right)^2 \right.$$
$$\left. \left. + (1-\nu)\pi^4 \left(\frac{h}{L} \right)^4 \right] \right] \sin \frac{\pi x}{L} \tag{30}$$

For the stress component σ_x, the classical, the shear deformation Reissner, the Essenburg, and the Level (2) theories all give the same results,

$$\sigma_x = 12 \frac{q_o}{\pi^2} \left(\frac{L}{h} \right)^2 \frac{z}{h} \sin \frac{\pi x}{L} \tag{31}$$

19

DISCUSSION

Through comparison with an exact solution, we seek to determine the relative accuracy of the various approximate theories, including the one presented herein. Due to the high order of the terms included in the present theory, it is of course not convenient to use. Accordingly, it would be helpful to deduce guidelines by which one can ascertain when it is necessary to use a high order theory, as given here, and when a lower order theory will suffice.

The range of theories to be considered are from the classical case to the present form. In between these extremes, the well-known Reissner shear deformation theory will be considered along with the extension of it by Essenburg to include transverse normal strain effects. Essenburg's theory employs assumptions upon both stresses and displacements. The Level (2) theory referred to in the previous section uses exactly the same assumuptions upon displacement as in Essenburg's theory; however, no corresponding assumptions are made upon the stresses. Rather, the Level (2) theory solution is obtained as a special case of that given herein, which of course is derived directly from potential energy. Thus, the Essenburg theory and the Level (2) theory are of the same order, but involve different derivations, and it will be of interest to compare them directly with each other.

Stress distributions across the thickness of the plate are displayed in Figure 1 for $h/L = 1.5$, where L is the half wave length of the sinusoidal loading pattern. Thus, the ordinate, h/L, is the ratio of thickness of plate to characteristic length of the loading

pattern. The high order theory due to Reissner corresponding to Level (4) is of the same order as the present theory based upon (5), the difference being that Reissner's theory omits the combined effects between in-plane and out-of-plane deformation modes. Thus, the Reissner Level (4) theory of necessity produces antisymmetric stress states about the middle plane of the plate. From Fig. 1 it is seen that the exact solution deviates strongly from the anti-symmetry characteristics just mentioned; thus it is clear that a theory of the type of (4) could not come close to reproducing the exact solution. Also, it is obvious from Figure 1 that the Reissner Level (1) and the Essenburg theories provide no improvement over the classical theory in terms of the accuracy of the stress representation. Considering the complex shape of the exact solution stress distribution, the present high order theory provides an effective modeling result.

The maximum value of stress σ_x (flexural stress) is plotted against h/L in Figure 2. Clearly, when the ratio of the thickness to the characteristic length of the load is of the order of 1, the present high order theory is needed to properly model the deformation effects in the plate and lower order theories are inadequate. This specific conclusion of course applies only to the present example, but we speculate that in all problems where disturbing features have a characteristic length of the order of the thickness, then a theory at least of the order of the present one would be required to properly model effects.

The maximum displacement of the middle plane of the plate according to the various theories are compared with the exact result in Figure 3.

21

It is seen that for h/L = 1.5 the deviations between the approximate

theories and the exact result are substantial, and the deviations

continue to increase with increasing h/L. The present high order

theory is seen giving the result closest to the exact result. The

results from Essenburg's theory and the Level (2) theory are of about

the same level of accuracy as one would expect for the reasons described

above. Note also that the present high order theory is clearly superior

to the Level (2) theory.

The main result of the present work is viewed as a complement to

the result found by Reissner [9], this result being that a theory of

the level of (4) or (5) is needed, in general, to provide a significant

improvement in the level of accuracy over that afforded by the classical

theory of plate deformation. Further, it follows that with a theory

of the level of (4) or (5), very accurate results can be obtained.

It is now possible to answer the question raised in the Introduction

of whether in a given problem the coupling effects implicit in (5) are

needed rather than using the simpler form (4). In the example studied

by Reissner [9] of the bending of an infinite plate with a circular

hole, the results derived from a theory corresponding to (4) were

entirely satisfactory and sufficient, whereas in the present example

the theory based upon (5) is required for the reasons described above.

An examination of the governing set of differential equations (6) shows

that the sets of equations governing the in-plane and the out-of-plane

deformation modes completely decouple. In the problem studied by

Reissner [9], the in-plane contributions to the problem are easily

shown to vanish identically, thus a theory based upon (5) provides no

22

new information over one based upon (4) in that problem. However, in the present problem the in-plane contribution to the solution has been shown to be significant, and cannot be neglected. Thus, it is seen that for plate bending problems where the loading characteristics possess a high degree of asymmetry, with respect to the middle plane, then a theory of the type of (5) rather (4) is required, while problems with loading characteristics which are close to being anti-symmetrical with respect to the middle plane then a theory of the type of (4) is sufficient. The bending of an infinite plate with a circular hole is an example of the latter type of problem, while the problem considered herein as well as contact problems, are examples of the former type. Of course, neither type of high order theory is needed unless the disturbing feature of geometry or the characteristic load length are of the order of the plate thickness.

Finally, it is appropriate to mention the nature of the stress resultants involved in the present theory. As seen from (7) - (9), there are resultants of higher order than bending moments and shear force involved in the governing differential equations. These same higher order resultants are also necessarily involved in the specification of edge conditions. It is logical to ask what is the significance of such high order resultants in edge condition specifications, and is there any way to avoid involvement with them. The answer to this question is very simple. There is no way to avoid consideration of these high order resultants in the present context; indeed, it would be disturbing if the present high order theory did not require the specification of corresponding high order resultants

23

along edges. For traction-free edges, of course, the resultants of all orders simply vanish. For loaded edges, the distribution of tractions across the thickness must be obtained or assumed, from which the resultants of all orders can be determined.

The extension of the present plate theory to laminated plate conditions is of particular importance since it is known that for laminates the distribution of in-plane displacements across the thickness may be strongly nonlinear. This extension is presented in Chapter II of this same work.

REFERENCES

1. E. Reissner - On the Theory of Bending of Elastic Plates, J. Math. Phys., Vol. 23, 1944, pp. 184-191.

2. E. Reissner - The Effects of Transverse Shear Deformation on the Bending of Elastic Plates, J. Appl. Mech., Vol. 12, No. 2, Trans. ASME, Vol. 67, June 1945, pp. 69-77.

3. R. D. Mindlin - Influence of Rotatory Inertia and Shear on Flexural Motions of Isotropic, Elastic Plates, J. Appl. Mech., Vol. 18, No. 1, Trans. ASME, Vol. 73, Mar. 1951, pp. 31-38.

4. P. M. Naghdi - On the Theory of Thin Elastic Shells, J. Appl. Math., Vol. 14, 1957, pp. 369-380.

5. F. Essenburg - On the Significance of the Inclusion of the Effect of Transverse Normal Strain in Problems Involving Beams with Surface Constraints, J. Appl. Mech., Vol. 42, Mar. 1975, pp. 127-132.

6. J. M. Whitney and C. T. Sun - A Refined Theory for Laminated Anisotropic, Cylindrical Shells, J. Appl. Mech., Vol. 41, June 1974, pp. 471-476.

7. R. B.Nelson and D. R. Lorch - A Refined Theory of Laminated Orthotropic Plates, J. Appl. Mech., Vol. 41, Mar. 1974, pp. 177-183.

8. F. B. Hildebrand, E. Reissner, and G. B. Thomas - Notes on the Foundations of the Theory of Small Displacements of Orthotropic Shells, NACA T. N. No. 1833, 1949.

9. E. Reissner - On Transverse Bending of Plates, Including the Effects of Transverse Shear Deformation, Int. J. Solids Structures, Vol. 11, 1975, pp. 569-573.

10. R. W. Little - Elasticity, Prentice-Hall, Inc., 1973, pp. 109-112.

FIGURE CAPTIONS

Figure 1: Flexural stress distributions for $\nu = 0.25$ and $h/L = 1.5$.

Figure 2: Maximum flexural stress distributions for $\nu = 0.25$.

Figure 3: Mid-plane displacement solution for $\nu = 0.25$.

26

(1) CLASSICAL, REISSNER LEVEL (1), ESSENBURG LEVEL (2) THEORIES

(2) EXACT SOLUTION

(3) PRESENT THEORY

Figure 1.

27

(1) CLASSICAL, REISSNER LEVEL (1),
    ESSENBURG LEVEL (2) THEORIES
(2) EXACT SOLUTION
(3) PRESENT THEORY

Figure 2.   28

$w° = $ DISPLACEMENT COEFFICIENT $\cdot \frac{q_0}{D} \cdot \frac{L^4}{\pi^4} \sin \frac{\pi x}{L}$

(1) CLASSICAL THEORY
(2) EXACT SOLUTION
(3) REISSNER LEVEL (1) THEORY
(4) LEVEL (2) THEORY
(5) PRESENT THEORY
(6) ESSENBURG'S THEORY

Figure 3.

29
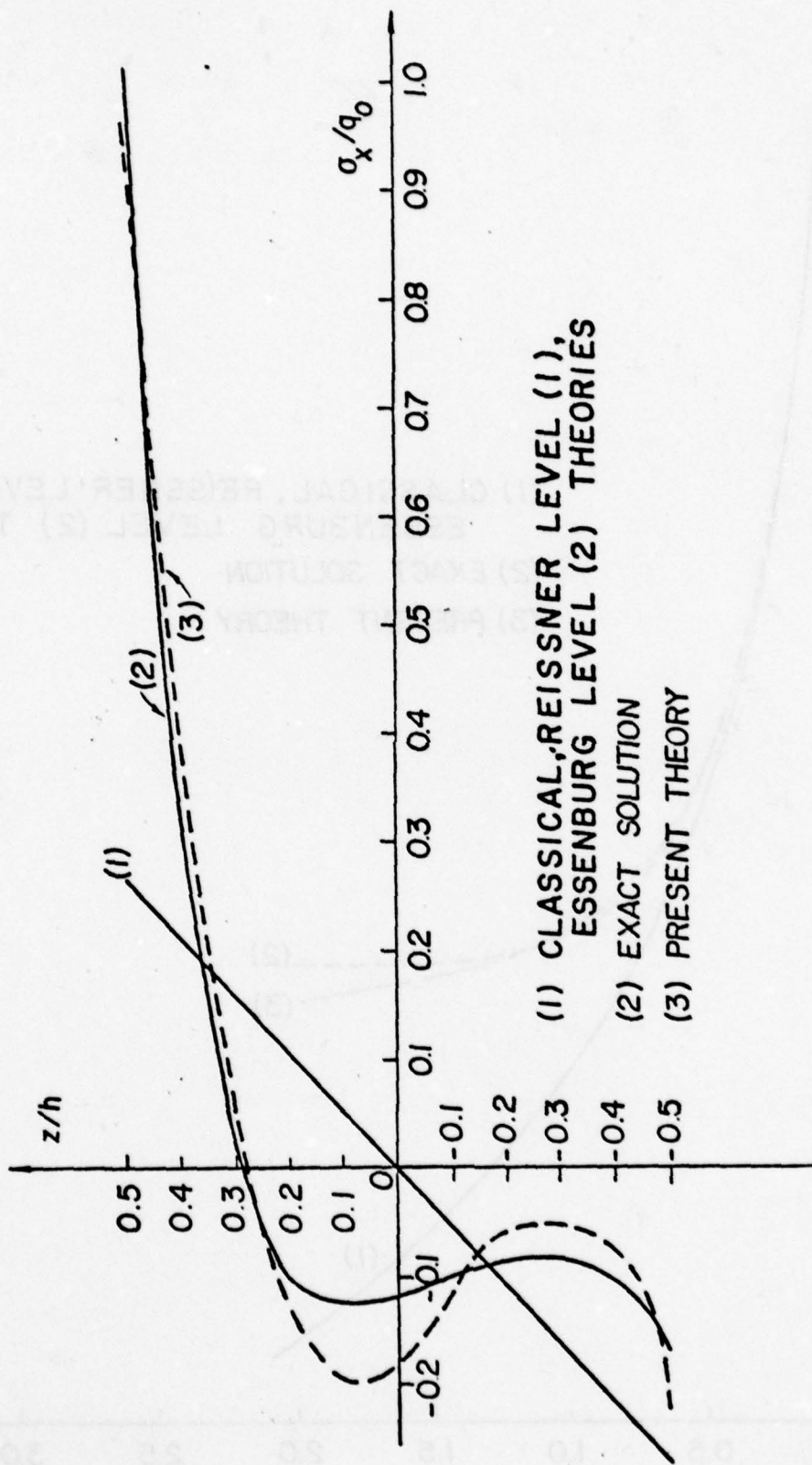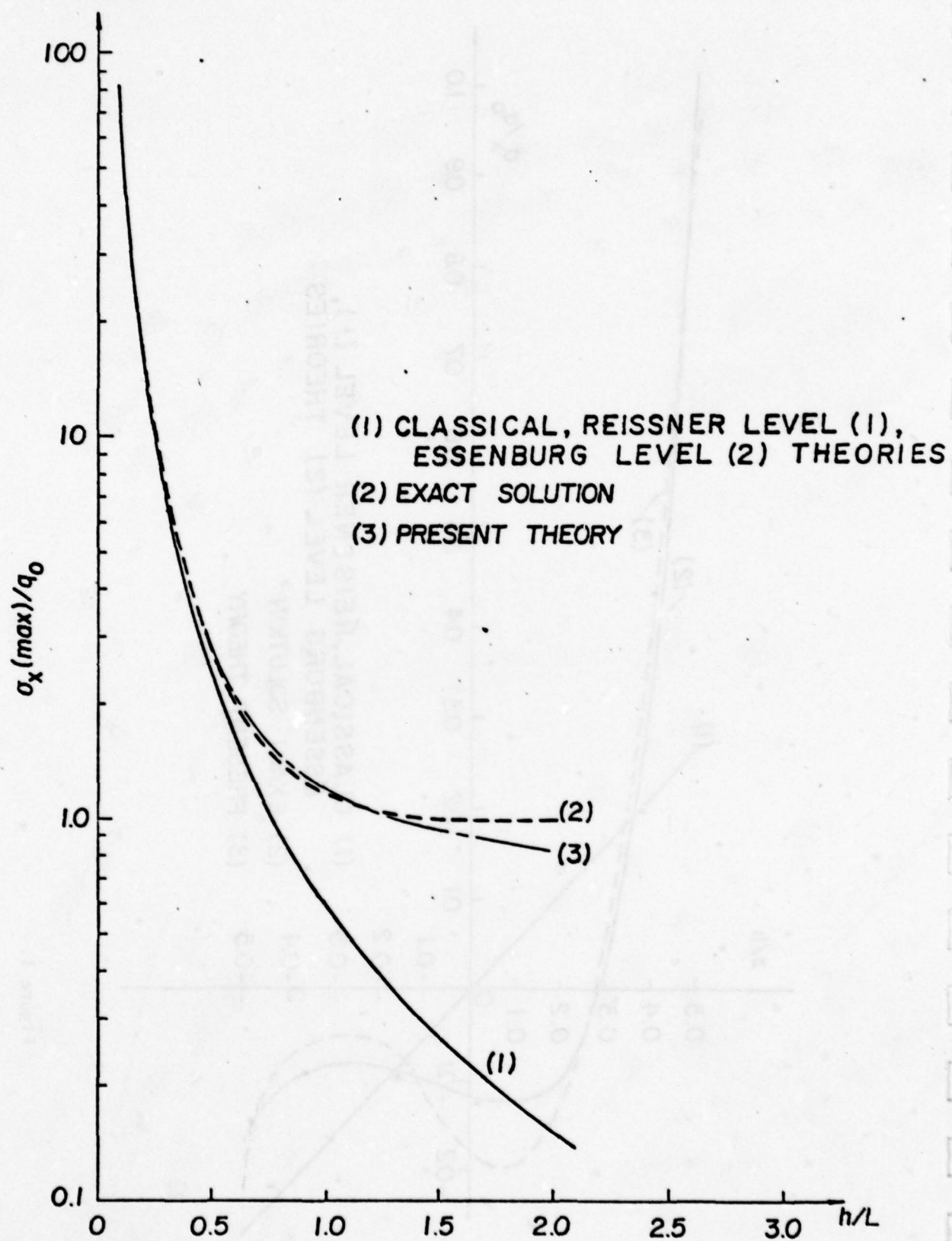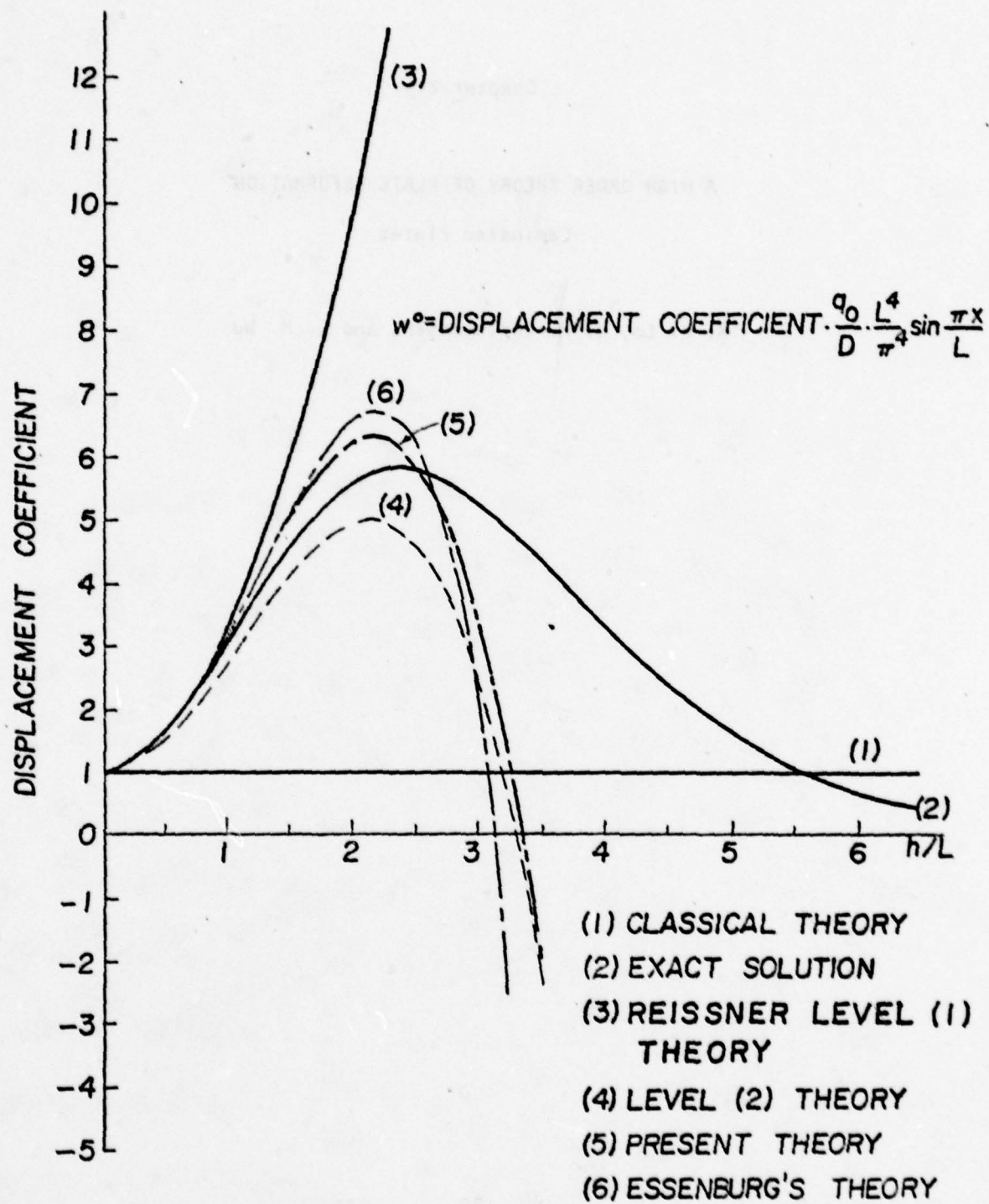
Chapter 2

A HIGH ORDER THEORY OF PLATE DEFORMATION
Laminated Plates

K. H. Lo, R. M. Christensen, and E. M. Wu

30
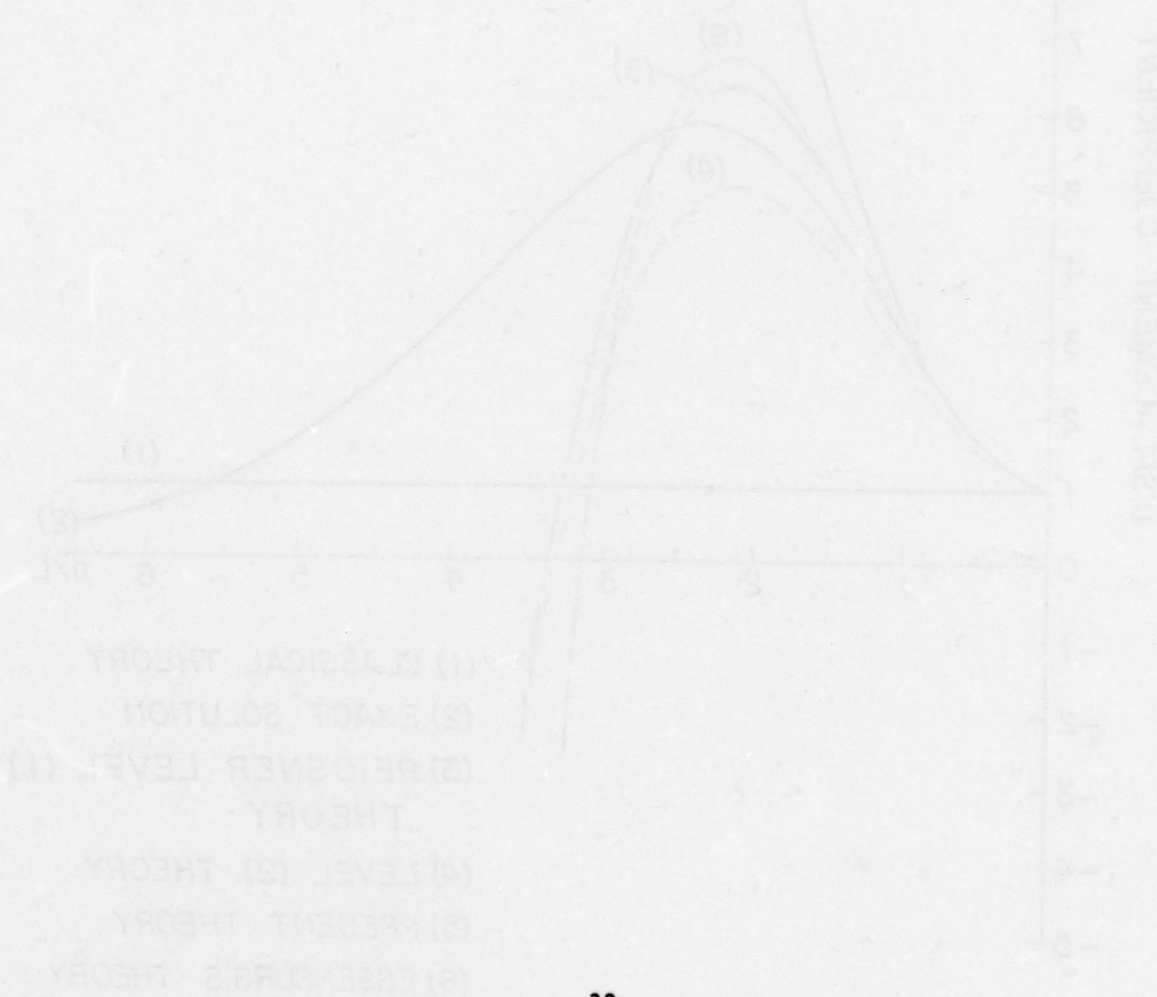
ABSTRACT

The high order theory of plate deformation developed in Chapter I of this work is extended here to model the behavior of laminated plates. Through comparison with elasticity solutions, it is shown the present theory correctly models effects not attainable from the classical theory.

INTRODUCTION

With the increasing use of composite materials in thick laminated form, the need for advanced methods of analysis is obvious. For such laminated systems, the components of stress and strain transverse to the plane of the laminate strongly influence the behavior. Thus, classical laminated plate theory, which is not formulated to account for the effect of these transverse stress and strain components, is not applicable to thick laminates. A high order theory of plate behavior is herein developed for application to laminates; this theory is an extension of that developed in Part I of this work [1], for application to homogeneous plates.

Many different high order laminated plate theories have been proposed which are intended to improve upon the classical laminated plate theory by accounting for the effects of the transverse components of strain in the plate. Typical examples of such theories are cited in [2-5]. The simplest of all the improved laminated theories are the ones based on an assumed displacement field of the form

$$u = u^\circ (x,y,t) + Z\psi_x(x,y,t)$$
$$v = v^\circ (x,y,t) + Z\psi_y(x,y,t) \qquad (1)$$
$$w = w (x,y,t)$$

31

Actually, relations (1) apply to both the classical form and the improved shear deformation theory, the difference being that in the classical theory the ψ_x and ψ_y terms are directly specified in terms of derivatives of w. Despite the increased generality of the shear deformation theory, the related flexural stress distributions show little improvement over those of the classical laminated plate theory. It is apparent that higher order terms are needed in the power series expansions of the assumed displacement field to properly model the behavior of the laminates.

In this paper, a consistent high order laminated plate theory is derived for the flexural behavior of laminated plates. The following displacement field is assumed:

$$u = u^\circ (x,y) + z\psi_x (x,y) + z^2 \zeta_x (x,y) + z^3\phi_x (x,y)$$

$$v = v^\circ (x,y) + z\psi_y (x,y) + z^2 \zeta_y (x,y) + z^3\phi_y (x,y) \qquad (2)$$

$$w = w^\circ (x,y) + z\psi_z (x,y) + z^2 \zeta_z (x,y)$$

The level of truncation in Equations (2) is consistent in the sense that the transverse shear strains due to in-plane displacements u and v are of the same order in z as those determined by the transverse displacement w. This high order laminated plate theory is an extension of the thick plate theory developed earlier for homogeneous isotropic plates [1]. The accuracy of the theory is assessed through its application to the problems of a bi-directional and an angle-ply laminate subjected to sinusoidal surface loading.

32

In addition to surface loading problems, there are other classes of problems of practical interest which require the use of a theory of the order of the one given herein. For example, stress risers such as cut-outs, loaded holes and subsurface cracks, and problems involving the impact of laminates by foreign objects cause stress distributions and localized stress gradients through the thickness of the plate that are essentially three-dimensional in nature and require the application of a high order theory.

LAMINATED PLATE THEORY

The theory used in this paper is based on the assumed displacement field as given in Equations (2). The constitutive relations for any layer of the laminate are of the form

$$
\begin{bmatrix} \sigma_x \\ \sigma_y \\ \sigma_z \\ \tau_{xy} \end{bmatrix} = \begin{bmatrix} C_{11} & C_{12} & C_{13} & C_{16} \\ C_{12} & C_{22} & C_{23} & C_{26} \\ C_{13} & C_{23} & C_{33} & C_{36} \\ C_{16} & C_{26} & C_{36} & C_{66} \end{bmatrix} \begin{bmatrix} \varepsilon_x \\ \varepsilon_y \\ \varepsilon_z \\ \gamma_{xy} \end{bmatrix}
$$

$$
\begin{bmatrix} \tau_{yz} \\ \tau_{xz} \end{bmatrix} = \begin{bmatrix} C_{44} & C_{45} \\ C_{45} & C_{55} \end{bmatrix} \begin{bmatrix} \gamma_{yz} \\ \gamma_{xz} \end{bmatrix}
$$

(3)

where C_{ij} are the components of the anisotropic stiffness matrix. It should be noted that all the six components of stress and strain tensors are included in this theory.

33

The governing equations pertinent to this theory are derived using the principle of stationary potential energy in the same manner as that in Ref. [1]. Eleven equilibrium equations are obtained for the determination of the eleven generalized displacement coefficients in Eqs. (2). The details of the derivations are omitted here; suffice it to say in full form the derivation is rather lengthy. These governing equations are recorded here, in an archive journal, for possible future use in related problems.

Governing equilibrium equations of higher order plate theory are given by

$$N_{x,x} + N_{xy,y} + q_x = 0$$

$$N_{y,y} + N_{xy,x} + q_y = 0$$

$$Q_{x,x} + Q_{y,y} + q = 0$$

$$M_{x,x} + M_{xy,y} - Q_x + m_x = 0$$

$$M_{y,y} + M_{xy,x} - Q_y + m_y = 0$$

$$R_{x,x} + R_{y,y} - N_z + m = 0$$

$$P_{x,x} + P_{xy,y} - 2R_x + n_x = 0$$

$$P_{y,y} + P_{xy,x} - 2R_y + n_y = 0$$

$$S_{x,x} + S_{y,y} - 2M_z + n = 0$$

$$\overline{M}_{x,x} + \overline{M}_{xy,y} - 3S_x + \ell_x = 0$$

$$\overline{M}_{y,y} + \overline{M}_{xy,x} - 3S_y + \ell_y = 0$$

(4)

where

$$\begin{bmatrix} N_x & N_y & N_z & N_{xy} & Q_x & Q_y \\ M_x & M_y & M_z & M_{xy} & R_x & R_y \end{bmatrix} = \int_{-h/2}^{h/2} \begin{Bmatrix} 1 \\ z \end{Bmatrix} [\sigma_x \ \sigma_y \ \sigma_z \ \tau_{xy} \ \tau_{xz} \ \tau_{yz}] dz$$

$$\begin{bmatrix} P_x & P_y & P_{xy} \\ \overline{M}_x & \overline{M}_y & \overline{M}_{xy} \end{bmatrix} = \int_{-h/2}^{h/2} \begin{Bmatrix} z^2 \\ z^3 \end{Bmatrix} (\sigma_x \ \sigma_y \ \tau_{xy}) \ dz \tag{5}$$

and

$$[S_x \quad S_y] = \int_{-h/2}^{h/2} z^2 \ (\tau_{xz} \ \tau_{yz}) \ dz$$

are the force resultants appropriate to this theory and

$$(q_x \quad n_x) = [\tau_{xz}(h/2) - \tau_{xz}(-h/2)] \ [1 \quad h^2/4]$$

$$(q_y \quad n_y) = [\tau_{yz}(h/2) - \tau_{yz}(-h/2)] \ [1 \quad h^2/4] \tag{6}$$

$$(m_x \quad \ell_x) = [\tau_{xz}(h/2) + \tau_{xz}(-h/2)] \ [h/2 \quad h^3/8]$$

$$(m_y \quad \ell_y) = [\tau_{yz}(h/2) + \tau_{yz}(-h/2)] \ [h/2 \quad h^3/8]$$

$$(q \quad n) = [\sigma_z(h/2) - \sigma_z(-h/2)] \ [1 \quad h^2/4]$$

$$m = \frac{h}{2} \ [\sigma_z(h/2) + \sigma_z(-h/2)]$$

35

Along the edge of the plate, one member of each of the following eleven products must be prescribed:

$$N_n \, u^\circ_n, \quad N_{nt} \, u^\circ_t, \quad M_n \, \psi_n$$

$$M_{nt} \, \psi_t, \quad P_n \, \zeta_n, \quad P_{nt} \, \zeta_t$$

$$\overline{M}_n \, \phi_n, \quad \overline{M}_{nt} \, \phi_t, \quad Q_n w^\circ \tag{7}$$

$$R_n \, \psi_z \quad \text{and} \quad S_n \, \zeta_z$$

where n and t are the directions normal and tangential to the edge of the plate.

The equations and boundary conditions given in (4)-(7) are independent of the properties of the materials of the plate and hence hold true for homogeneous isotropic as well as laminated plates.

Next, the governing equilibrium equations are expressed in terms of the displacement coefficients.

Using Eqns. (2), (4), (5) and strain-displacement relations, the governing equilibrium equations can be written in the following form:

$$
\left[L_{i,j} \right]
\begin{bmatrix}
u^\circ \\
v^\circ \\
w^\circ \\
\psi_x \\
\psi_y \\
\psi_z \\
\zeta_x \\
\zeta_y \\
\zeta_z \\
\phi_x \\
\phi_y
\end{bmatrix}
= -
\begin{bmatrix}
q_x \\
q_y \\
-q \\
m_x \\
m_y \\
-m \\
n_x \\
n_y \\
-n \\
\ell_x \\
\ell_y
\end{bmatrix}
\tag{8}
$$

36

where the operators $L_{i,j}$ are symmetric and have the following forms

$$
\begin{bmatrix} L_{1,1} \\ L_{1,2} \\ L_{1,4} \\ L_{1,5} \\ L_{1,7} \\ L_{1,8} \\ L_{1,10} \\ L_{1,11} \end{bmatrix} = \begin{bmatrix} A_{11} \\ A_{16} \\ B_{11} \\ B_{16} \\ D_{11} \\ D_{16} \\ F_{11} \\ F_{16} \end{bmatrix} [\ ]_{,xx} + \begin{bmatrix} 2A_{16} \\ A_{12} + A_{66} \\ 2B_{16} \\ B_{12} + B_{66} \\ 2D_{16} \\ D_{12} + D_{66} \\ 2F_{16} \\ F_{12} + F_{66} \end{bmatrix} [\ ]_{,xy} + \begin{bmatrix} A_{66} \\ A_{26} \\ B_{66} \\ B_{26} \\ D_{66} \\ D_{26} \\ F_{66} \\ F_{26} \end{bmatrix} [\ ]_{,xy}
$$

$$L_{1,3} = 0$$

$$
\begin{bmatrix} L_{1,6} \\ L_{1,9} \end{bmatrix} = \begin{bmatrix} A_{13} \\ 2B_{13} \end{bmatrix} [\ ]_{,x} + \begin{bmatrix} A_{36} \\ 2B_{36} \end{bmatrix} [\ ]_{,y}
$$

$$L_{2,3} = 0, \quad L_{2,4} = L_{1,5}, \quad L_{2,7} = L_{1,8}, \quad L_{2,10} = L_{1,11}$$

$$
\begin{bmatrix} L_{2,2} \\ L_{2,5} \\ L_{2,8} \\ L_{2,11} \end{bmatrix} = \begin{bmatrix} A_{66} \\ B_{66} \\ D_{66} \\ F_{66} \end{bmatrix} [\ ]_{,xx} + 2 \begin{bmatrix} A_{26} \\ B_{26} \\ D_{26} \\ F_{26} \end{bmatrix} [\ ]_{,xy} + \begin{bmatrix} A_{22} \\ B_{22} \\ D_{22} \\ F_{22} \end{bmatrix} [\ ]_{,yy}
$$

37

$$\begin{bmatrix} L_{2,6} \\ L_{2,9} \end{bmatrix} = \begin{bmatrix} A_{36} \\ 2B_{36} \end{bmatrix} [\ ]_{,x} + \begin{bmatrix} A_{23} \\ 2B_{23} \end{bmatrix} [\ ]_{,y}$$

$$\begin{bmatrix} L_{3,3} \\ L_{3,6} \\ L_{3,9} \end{bmatrix} = \begin{bmatrix} -A_{55} \\ -B_{55} \\ -D_{55} \end{bmatrix} [\ ]_{,xx} + \begin{bmatrix} -2A_{45} \\ -2B_{45} \\ -2D_{45} \end{bmatrix} [\ ]_{,xy} + \begin{bmatrix} -A_{44} \\ -B_{44} \\ -D_{44} \end{bmatrix} [\ ]_{,y}$$

$$\begin{bmatrix} L_{3,4} \\ L_{3,5} \\ L_{3,7} \\ L_{3,8} \\ L_{3,10} \\ L_{3,11} \end{bmatrix} = \begin{bmatrix} -A_{55} \\ -A_{45} \\ -2B_{55} \\ -2B_{45} \\ -3D_{55} \\ -3D_{45} \end{bmatrix} [\ ]_{,x} + \begin{bmatrix} -A_{45} \\ -A_{44} \\ -2B_{45} \\ -2B_{44} \\ -3D_{45} \\ -3D_{44} \end{bmatrix} [\ ]_{,y}$$

$$L_{4,4} = L_{1,7} - A_{55} [\ ]$$

$$L_{4,5} = L_{1,8} - A_{45} [\ ]$$

$$L_{4,6} = (L_{1,9} + L_{3,7})/2$$

$$L_{4,7} = L_{1,10} - 2B_{55} [\ ]$$

$$L_{4,8} = L_{1,11} - 2B_{45} [\ ]$$

$$L_{4,9} = (2D_{13} - D_{55}) [\ ]_{,x} + (2D_{36} - D_{45}) [\ ]_{,y}$$

$$\begin{bmatrix} L_{4,10} \\ L_{4,11} \end{bmatrix} = \begin{bmatrix} H_{11} \\ H_{16} \end{bmatrix} [\ ]_{,xx} + \begin{bmatrix} 2H_{16} \\ H_{12}+H_{66} \end{bmatrix} [\ ]_{,xy} + \begin{bmatrix} H_{66} \\ H_{26} \end{bmatrix} [\ ]_{,yy} - 3 \begin{bmatrix} D_{55} \\ D_{45} \end{bmatrix} [\ ]$$

38

$$L_{5,5} = L_{2,8} - A_{44} [\ ]$$

$$L_{5,6} = (L_{2,9} + L_{3,8})/2$$

$$L_{5,7} = L_{4,8}$$

$$L_{5,8} = L_{2,11} - 2B_{44} [\ ]$$

$$L_{5,9} = (2D_{36} - D_{45}) [\ ]_{,x} + (2D_{23} - D_{44}) [\ ]_{,y}$$

$$L_{5,10} = L_{4,11}$$

$$L_{5,11} = H_{66} [\ ]_{,xx} + 2H_{26} [\ ]_{xy} + H_{22} [\ ]_{,yy} - 3D_{44} [\ ]$$

$$L_{6,6} = L_{3,9} + A_{33} [\ ]$$

$$\begin{bmatrix} L_{6,7} \\ L_{6,8} \\ L_{6,10} \\ L_{6,11} \end{bmatrix} = \begin{bmatrix} D_{13} - 2D_{55} \\ D_{36} - 2D_{45} \\ F_{13} - 3F_{55} \\ F_{36} - 3F_{45} \end{bmatrix} [\ ]_{,x} + \begin{bmatrix} D_{36} - 2D_{45} \\ D_{23} - 2D_{44} \\ F_{36} - 3F_{45} \\ F_{23} - 3F_{44} \end{bmatrix} [\ ]_{,y}$$

$$L_{6,9} = -F_{55} [\ ]_{,xx} - 2F_{45} [\ ]_{,xy} - F_{44} [\ ]_{,yy} + 2B_{33}$$

$$L_{7,7} = L_{4,10} - D_{55} [\ ]$$

$$L_{7,8} = L_{4,11} - D_{45} [\ ]$$

$$L_{7,9} = 2(F_{13} - F_{55}) [\ ]_{,x} + 2(F_{36} - F_{45}) [\ ]_{,y}$$

$$\begin{bmatrix} L_{7,10} \\ L_{7,11} \end{bmatrix} = \begin{bmatrix} K_{11} \\ K_{16} \end{bmatrix} [\ ]_{,xx} + \begin{bmatrix} 2K_{16} \\ K_{12}+K_{66} \end{bmatrix} [\ ]_{,xy} + \begin{bmatrix} K_{66} \\ K_{26} \end{bmatrix} [\ ]_{,yy} - 6 \begin{bmatrix} F_{55} \\ F_{45} \end{bmatrix} [\ ]$$

39

$$L_{8,8} = L_{5,11} - D_{44} [\ ]$$

$$L_{8,9} = 2(F_{36} - F_{45}) [\ ]_{,x} + 2(F_{23} - F_{44}) [\ ]_{,y}$$

$$L_{8,10} = L_{7,11}$$

$$L_{8,11} = K_{66} [\ ]_{,xx} + 2K_{26} [\ ]_{,xy} + K_{22} [\ ]_{,yy} - 6F_{44} [\ ]$$

$$L_{9,9} = -H_{55} [\ ]_{,xx} - 2H_{45} [\ ]_{,xy} - H_{44} [\ ]_{,yy} + 4D_{33}$$

$$\begin{bmatrix} L_{9,10} \\ L_{9,11} \end{bmatrix} = \begin{bmatrix} 2H_{13} - 3H_{55} \\ 2H_{36} - 3H_{45} \end{bmatrix} [\ ]_{,x} + \begin{bmatrix} 2H_{36} - 3H_{45} \\ 2H_{23} - 3H_{44} \end{bmatrix} [\ ]_{,y}$$

$$\begin{bmatrix} L_{10,10} \\ L_{10,11} \\ L_{11,11} \end{bmatrix} = \begin{bmatrix} \mathcal{L}_{11} \\ \mathcal{L}_{16} \\ \mathcal{L}_{66} \end{bmatrix} [\ ]_{,xx} + \begin{bmatrix} 2\mathcal{L}_{16} \\ \mathcal{L}_{12} + \mathcal{L}_{66} \\ 2\mathcal{L}_{26} \end{bmatrix} [\ ]_{,xy} + \begin{bmatrix} \mathcal{L}_{66} \\ \mathcal{L}_{26} \\ \mathcal{L}_{22} \end{bmatrix} [\ ]_{,yy} - 9 \begin{bmatrix} H_{55} \\ H_{45} \\ H_{44} \end{bmatrix} [$$

$$(9)$$

where the notation $[\ ]_{,xx}$ etc. refers to derivatives of the column matrix of generalized displacements shown in (8).

The coefficients A_{ij}, B_{ij}, D_{ij}, F_{ij}, H_{ij}, K_{ij} and $\mathcal{L}_{ij}$ are defined as follows

$$(A_{ij}, B_{ij}, D_{ij}, F_{ij}, H_{ij}, K_{ij}, \mathcal{L}_{ij}) = \int_{-h/2}^{h/2} (1, z, z^2, z^3, z^4, z^5, z^6) C_{ij} dz$$

$$(10)$$

For symmetric laminates, B_{ij}, F_{ij}, and K_{ij} are identically equal to zero.

Problems involving angle-ply and cross-ply laminates subjected
to static sinusoidal loadings are next used to assess the degree of
accuracy of this high order laminated plate theory.

NUMERICAL EXAMPLES

A. Angle-Ply Laminate

Consider an infinite angle-ply laminate of thickness, h, subjected
to a pressure on the top surface $z = h/2$ of the form

$$q = q_o \sin \frac{x}{L} \tag{11}$$

with all other surface tractions identically equal to zero. The problem
can be solved by assuming a solution of the form

$$u = (a_o + za_1 + z^2a_2 + z^3a_3) \cos \frac{\pi x}{L}$$

$$v = (b_o + zb_1 + z^2b_2 + z^3b_3) \cos \frac{\pi x}{L} \tag{12}$$

$$w = (c_o + zc_1 + z^2c_2) \sin \frac{\pi x}{L}$$

where the constants a_i, b_i, and c_i are determined by the satisfaction
of the governing equations given in the Appendix.

Numberical results for a three-layer symmetric laminate are shown
in Figures 1-4. The ply orientations and thickness are $(+30°, -30°, +30°)$
and $(h/4, h/2, h/4)$ respectively. The following properties are used for
each ply

41

$$E_L = 25 \times 10^6 \text{ psi}, \; E_T = 10^6 \text{ psi}$$

$$G_{LT} = 0.5 \times 10^6 \text{ psi}, \; G_{TT} = 0.2 \times 10^6 \text{ psi} \qquad (13)$$

$$\nu_{LT} = \nu_{TT} = 0.25$$

where L and T are the directions parallel and normal to the fibers, respectively, and ν_{LT} is the Poisson's ratio measuring transverse strain under normal stress parallel to the fibers. These are typical values of high modulus graphite/epoxy composites. The stress and displacement components in Figures 1-4 are normalized as follows

$$\bar{u} = \frac{100_T u}{q_o h S^3}$$

$$\qquad (14)$$

$$\bar{\sigma} = \frac{\sigma}{q_o S^2}, \; S = \frac{L}{h}$$

for comparison with the exact elasticity solutions given by Pagano [7].

Figures 1 and 2 show the flexural stress distributions for the case L/h = 10 and L/h = 4, respectively. The agreement with exact elasticity solution is exceptionally good in the region of high values of flexural stresses. As the interface between different layers is approached, the stresses in the +30° is slightly different from that given by exact elasticity solutions. However, such a slight difference is immaterial, especially at the regions of low values of stresses.

Figures 3 and 4 show the corresponding in-plane displacement in the x-direction. As in the case of flexural stresses, good agreement with exact elasticity solutions is observed. The solutions in Figures 3

42

and 4 reveal the necessity for modeling the nonlinear distribution of displacements.

B. Bidirectional Laminates

A more critical test of the laminated plate theory can be obtained by repeating the above problem for a symmetric bidirectional laminate. In this case a higher discontinuity in material properties is experienced at the interface of different layers. Numerical results for a three-layered (0°, 90°, 0°) bidirectional laminate are given in Figures 5 and 6 for the flexural stress distributions. The material properties in each layer are the same as given in Eqs. (13) and the results are compared with the exact elasticity solutions given by Pagano [8].

As in the case of angle-ply laminates, close agreement of the numerical results with exact elasticity solutions is obtained. The relatively large discrepancies in the values of the flexural stresses at the interface between different layers is due to the high discontinuity in the values of C_{11} across the interface of different layers. However, as before, such discrepancies occur in the regions of low values of flexural stresses where accurate predictions of flexural stresses are not important.

DISCUSSION

By comparing the results obtained with the exact elasticity solutions and the classical laminated plate solutions, it is obvious that the present high order laminated plate theory gives a much better approximation to the behavior of laminated plates. This is especially

43

true in the case of relatively thick laminates where the effects of the transverse components of stress and strain could not be neglected. As in Ref. [1], the present high order theory is expected to give reasonably accurate solutions for problems where the characteristic length of the loading pattern or the dimensions of the disturbing features, such as cut-outs, are of the order of thickness of the plate.

The laminate stiffness coefficients B_{ij}, F_{ij}, and K_{ij}, as given in Eq. (14) represent the coupling between the in-plane and out-of-plane response of the laminate. In the case of symmetric laminates, it can be seen from Eq. (14) that these coupling coefficinets are identically equal to zero. Thus, for symmetric laminates, the governing eleven equilibrium equations can be separated into a set of five second-order differential equations governing the in-plane displacement components of the laminate as given by

$$u = u^{\circ}(x,y) + z^2 \zeta_x(x,y)$$

$$v = v^{\circ}(x,y) + z^2 \zeta_y(x,)$$

(15)

$$w = z \psi_z(x,y)$$

and a set of six second order differential equations governing the flexural displacement components as given by

$$u = z \psi_x(x,y) + z^3 \phi_x(x,y)$$

$$v = z \psi_y(x,y) + z^3 \phi_y(x,y)$$

(16)

$$w = w^{\circ}(x,y) + z^2 \zeta_z(x,y)$$

44

For symmetric laminates subjected to loadings which also are symmetrical with respect to the middle plane of the laminate, Eqs. (15) provide an approximation to the in-plane response of the laminates, with no contribution coming from Eqs. (16).

Similarly, if the symmetric laminate is subjected only to anti-symmetrical loadings, Eqs. (16) provide an approximation to the flexural behavior of the laminate. For loadings which are neither symmetrical nor anti-symmetrical, terms from both Eqs. (15) and (16) will contribute to the total response of the laminate. For many problems, however, the in-plane contributions to the flexural behavior of symmetric laminates are small except for very thick laminates. To illustrate this, Fig. 7 gives the flexural stress distribution for a moderately thick symmetric angle-ply laminate based on Eqs. (2) and (16) for $L/h = 4$. As can be seen from the figures, the two different stress distributions are extremely close to each other. Based upon the results obtained in Part I, it would probably be at about $L/h = 1$ where the contributions from both Eqs. (15) and (16) are comparable.

For unsymmetric laminates, the coupling coefficients B_{ij}, F_{ij} and K_{ij} are not identically equal to zero and, hence, the in-plane and out-of-plane deformations are coupled with each other. The behavior of the laminate is thus determined by the solution of a set of eleven coupled second order partial differential equations. Figure 8 gives the flexural stress distributions for a [+30°, -30°, +30°, -30°, +30°, -30°] unsymmetric laminate subjected to a sinusoidal loading as specified by Eqs. (11). The corresponding solutions obtained by using Eqs. (16), i.e., neglecting the coupling effects of the in-plane

45

displacements components, are also given. From Fig. 8 it is seen that
the flexural stress distributions are strongly influenced by the effects
of in-plane coupling. In fact, the use of only the terms in (16) leads
to a solution which has a continuous flexural component of stress,
which as seen from Fig. 8, is completely erroneous. Thus, Eqs. (2)
must be used to obtain accurate stress distributions.

Finally, it should be mentioned that the present results were
obtained with no recourse to shear correction factors, which are
commonly employed in laminated plate analysis. As discussed in Chapter I
of this work, it would be inconsistent to employ these factors with a
high order theory of plate deformation.

REFERENCES

1. K. H. Lo, R. M. Christensen, and E. M. Wu - A High Order Theory of Plate Deformation, Part I: Homogeneous Plates. Submitted for Publication.

2. J. M. Whitney and N. J. Pagano - Shear Deformation in Heterogeneous Anisotropic Plates. J. Appl. Mech., Vol. 37, pp. 1031-1036.

3. J. M. Whitney - Stress Analysis of Thick Laminated Composite and Sandwich Plates. J. Comp. Mats., Vol. 6, 1972, pp. 426-440.

4. J. M. Whitney and C. T. Sun - A Higher Order Theory for Extensional Motion of Laminated Composites. J. Sound and Vibration, Vol. 30, 1973, pp. 85-97.

5. R. B. Nelson and D. R. Lorch - A Refined Theory of Laminated Orthotropic Plates. J. Appl. Mech. Vol. 41, 1974, pp. 177-183.

6. R. D. Mindlin - Influence of Rotatory Inertia and Shear on Flexural Motions of Isotropic, Elastic Plates. J. Appl. Mech., Vol. 18, 1951, pp. 31-38.

7. N. J. Pagano - Influence of Shear Coupling in Cylindrical Bending of Anisotropic Laminates. J. Comp. Mats.- Vol. 4, 1970, pp. 330-343.

8. N. J. Pagano - Exact Solutions for Composite Laminates in Cylindrical Bending. J. Comp. Mats., Vol. 3, 1969, pp. 398-411.

FIGURE CAPTIONS

Figure 1: Flexural stress distributions for $[+30°, -30°]_s$ angle-ply laminate at L/h = 10.0.

Figure 2: Flexural stress distributions for $[+30°, -30°]_s$ angle-ply laminate at L/h = 4.0.

Figure 3: In-plane displacement $\bar{u}$ for $[+30°, -3-°]_s$ angle-ply laminate at L/h = 10.0.

Figure 4: In-plane displacement $\bar{u}$ for $[+30°, -30°]_s$ angle-ply laminate at L/h = 4.0.

Figure 5: Flexural stress distributions for $[0°, 90°, 0°]$ cross-ply lamiante at L/h = 10.0.

Figure 6: Flexural stress distributions for $[0°, 90°, 0°]$ cross-ply laminate at L/h = 4.0.

Figure 7: Comparison of flexural stress distributions due to Eqs. (2) and (9) for $[+30°, -30°]_s$ angle-ply laminate at L/h = 4.

Figure 8: Comparison of flexural stress distributions due to Eqs. (2) and (9) for unsymmetric $[+30°, -30°, +30°, -30°, +30°, -30°]$ angle-ply laminate at L/h = 10.

48

Figure 1.

EXACT ELASTICITY SOLUTION
HIGHER ORDER LAMINATED PLATE THEORY
CLASSICAL LAMINATED PLATE THEORY

$(L/h) = 4$

Figure 2.

50

Figure 3.

51
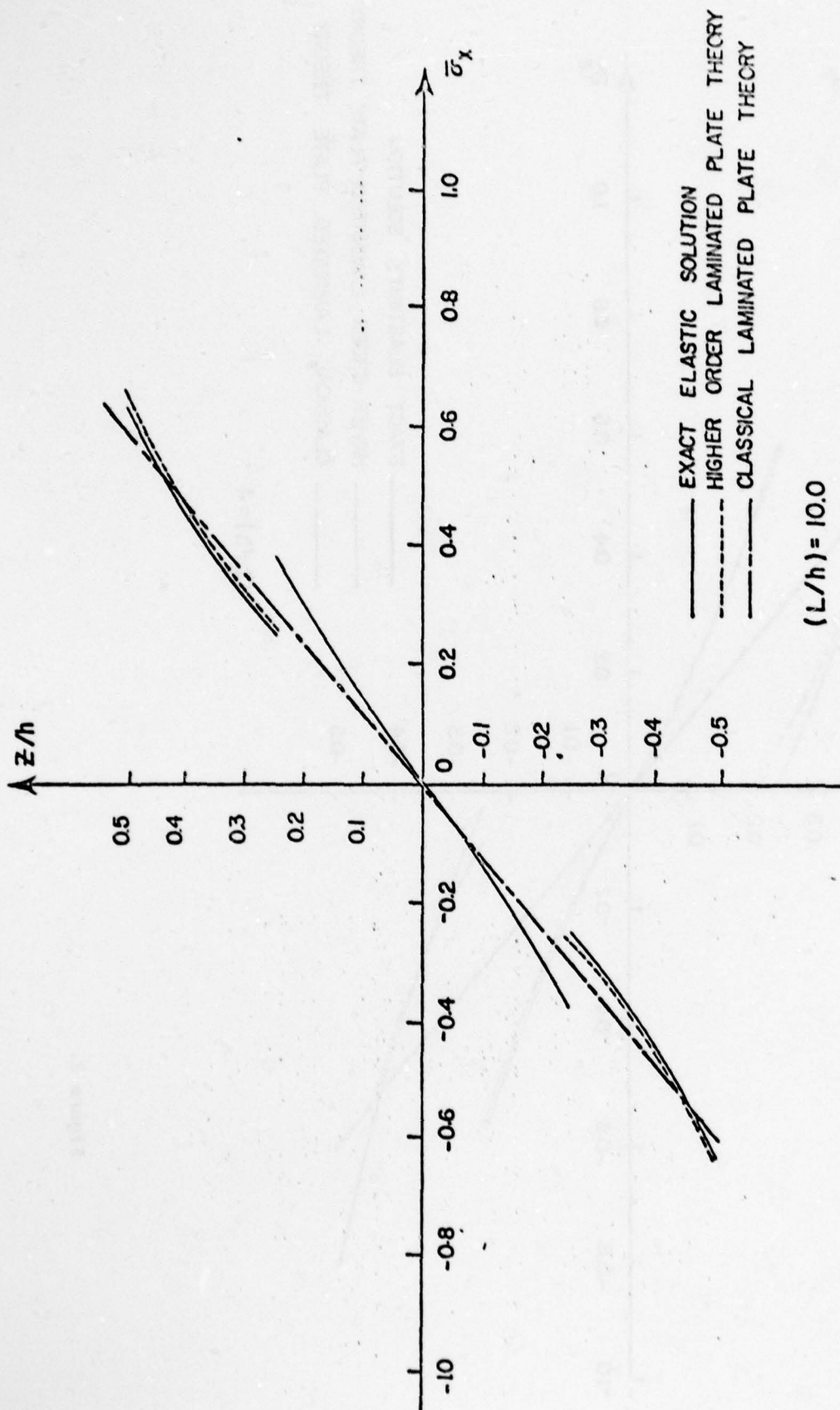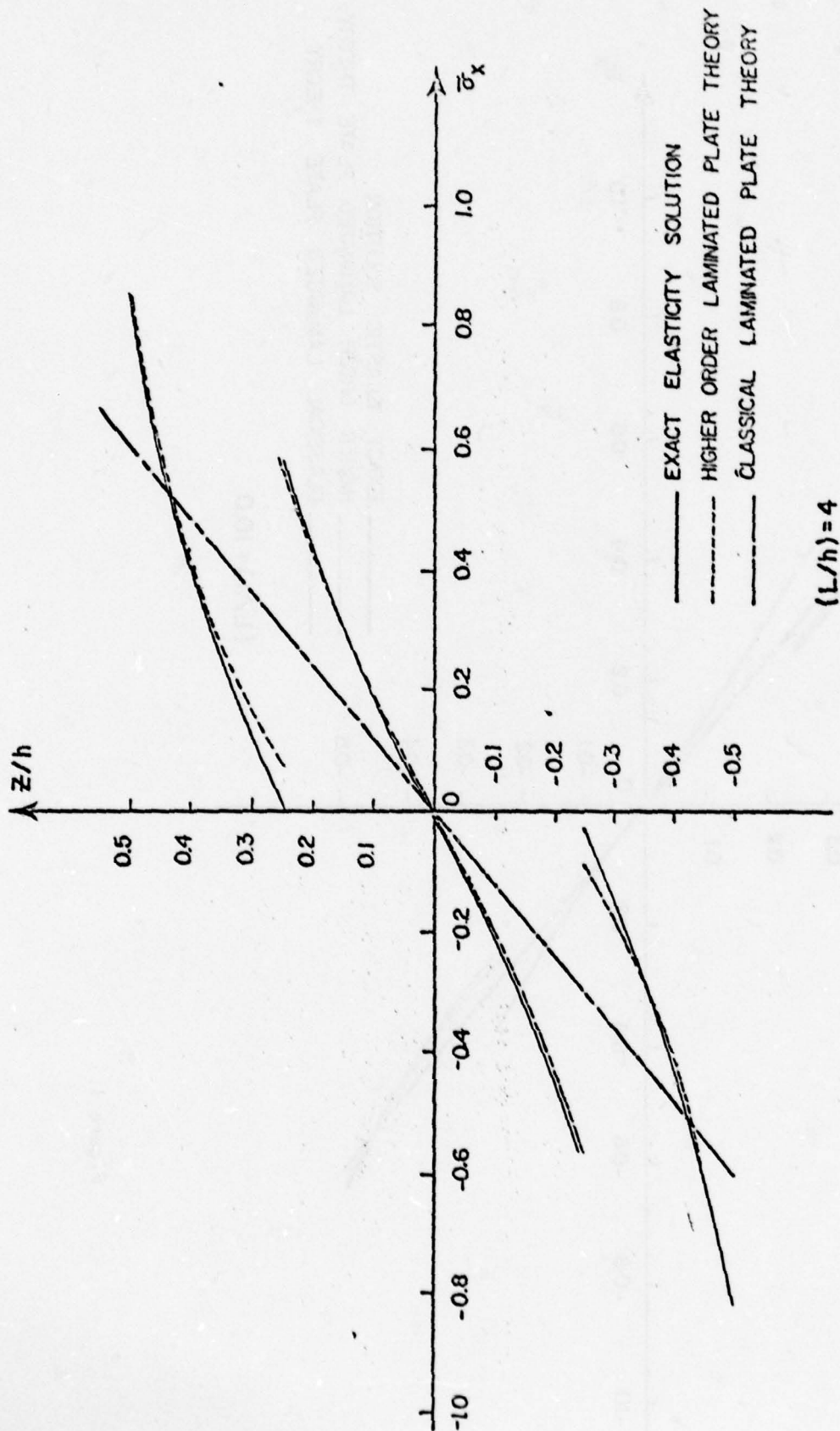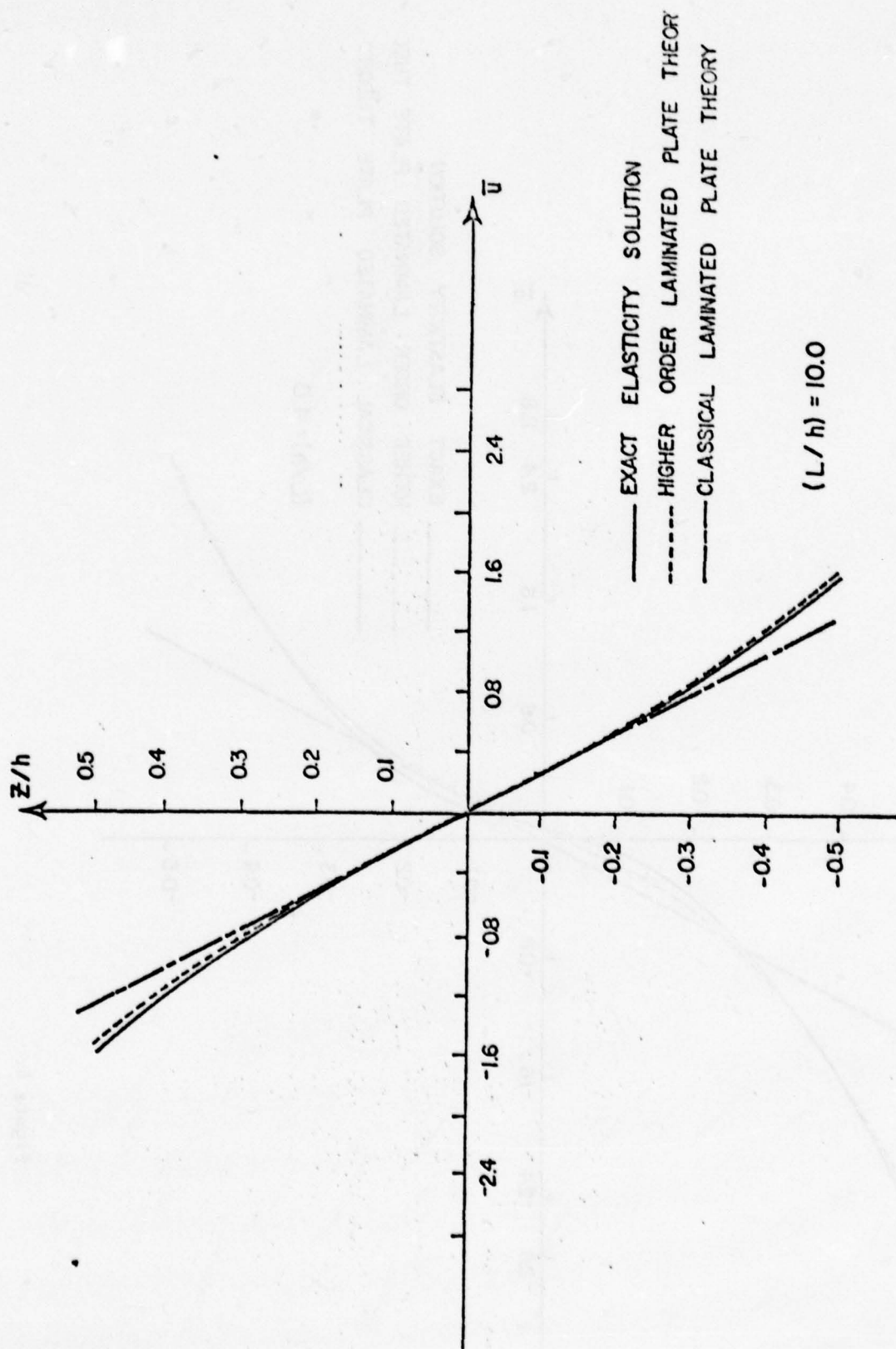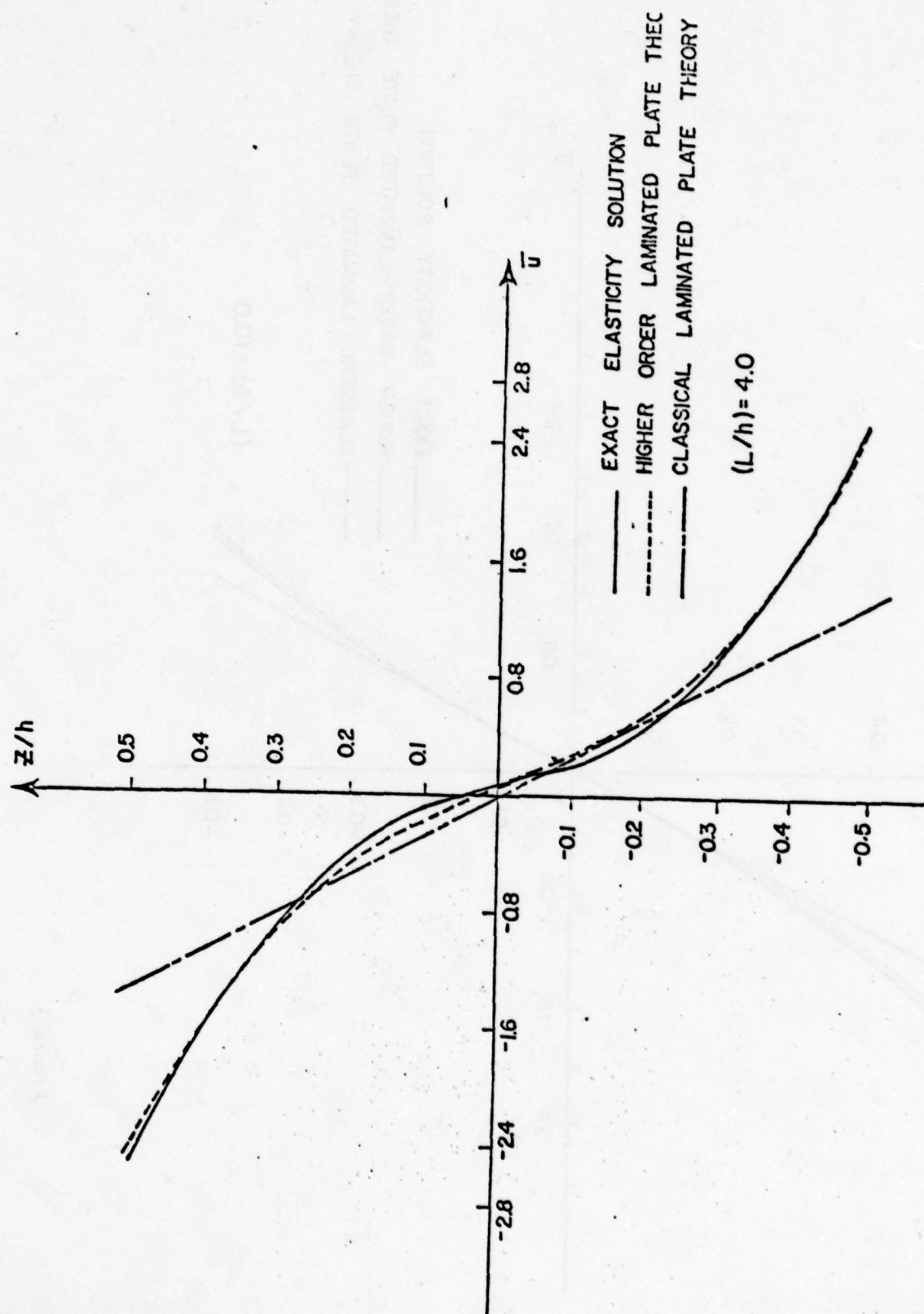
Figure 4.

Figure 5.

Figure 6.

54
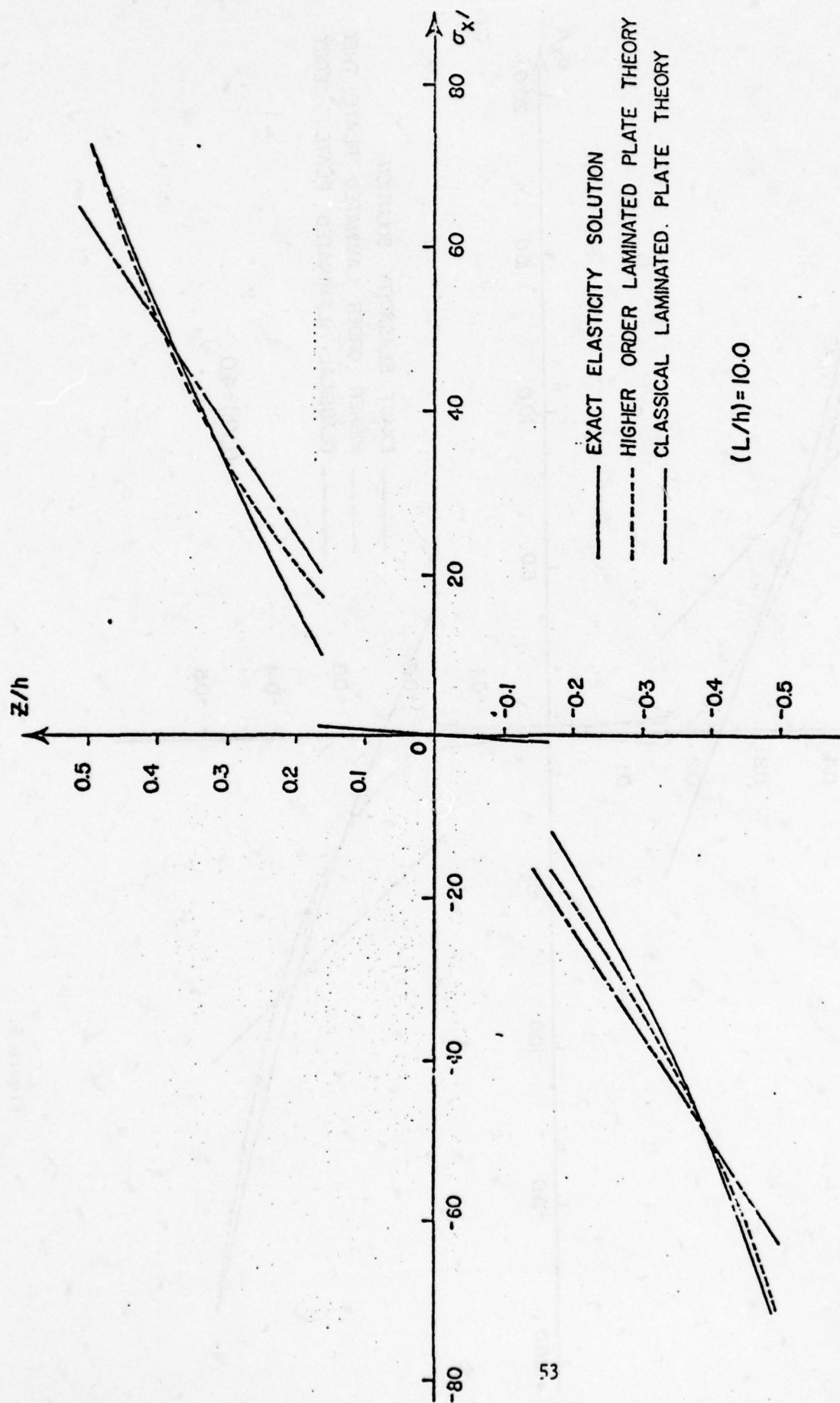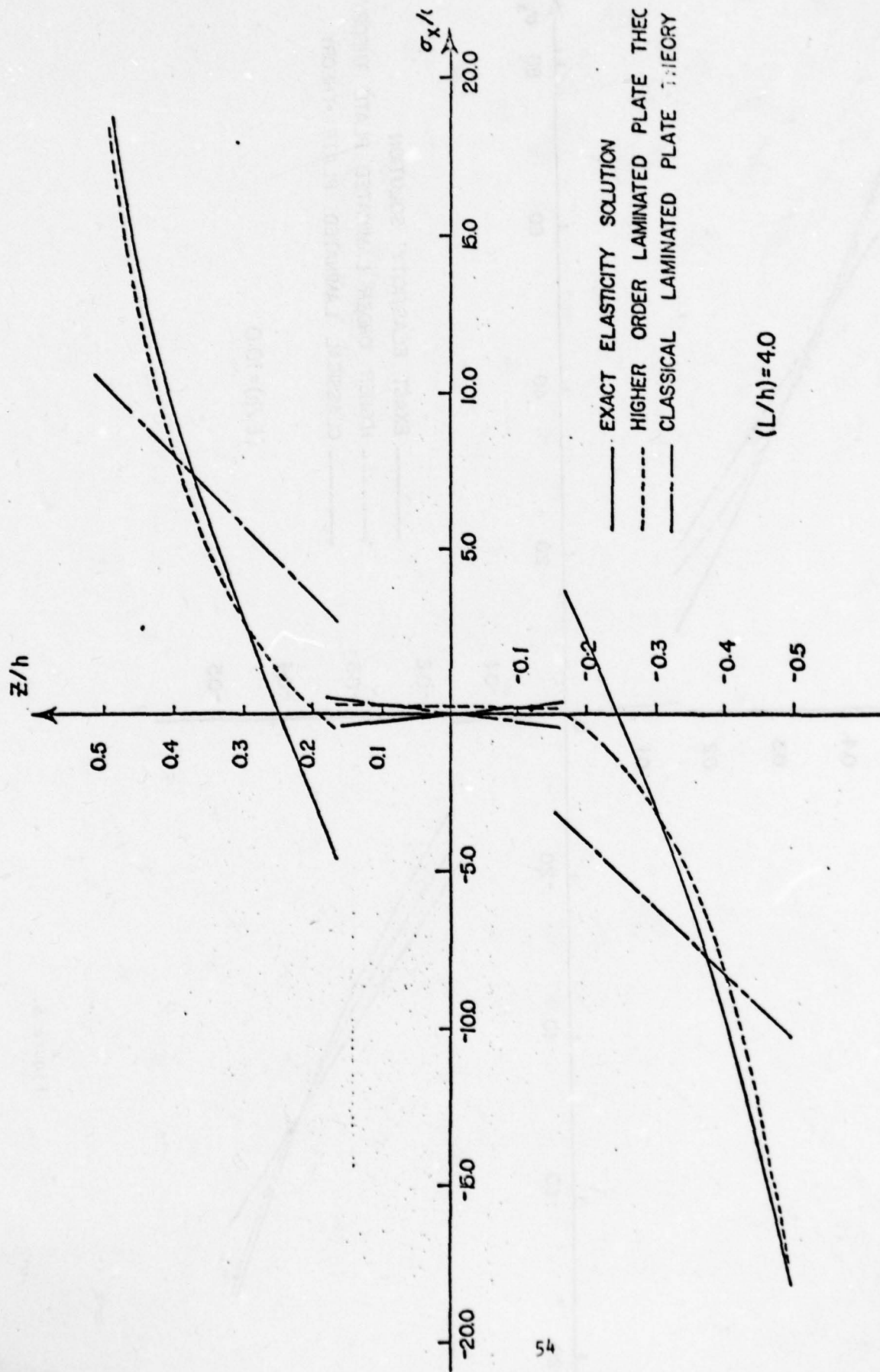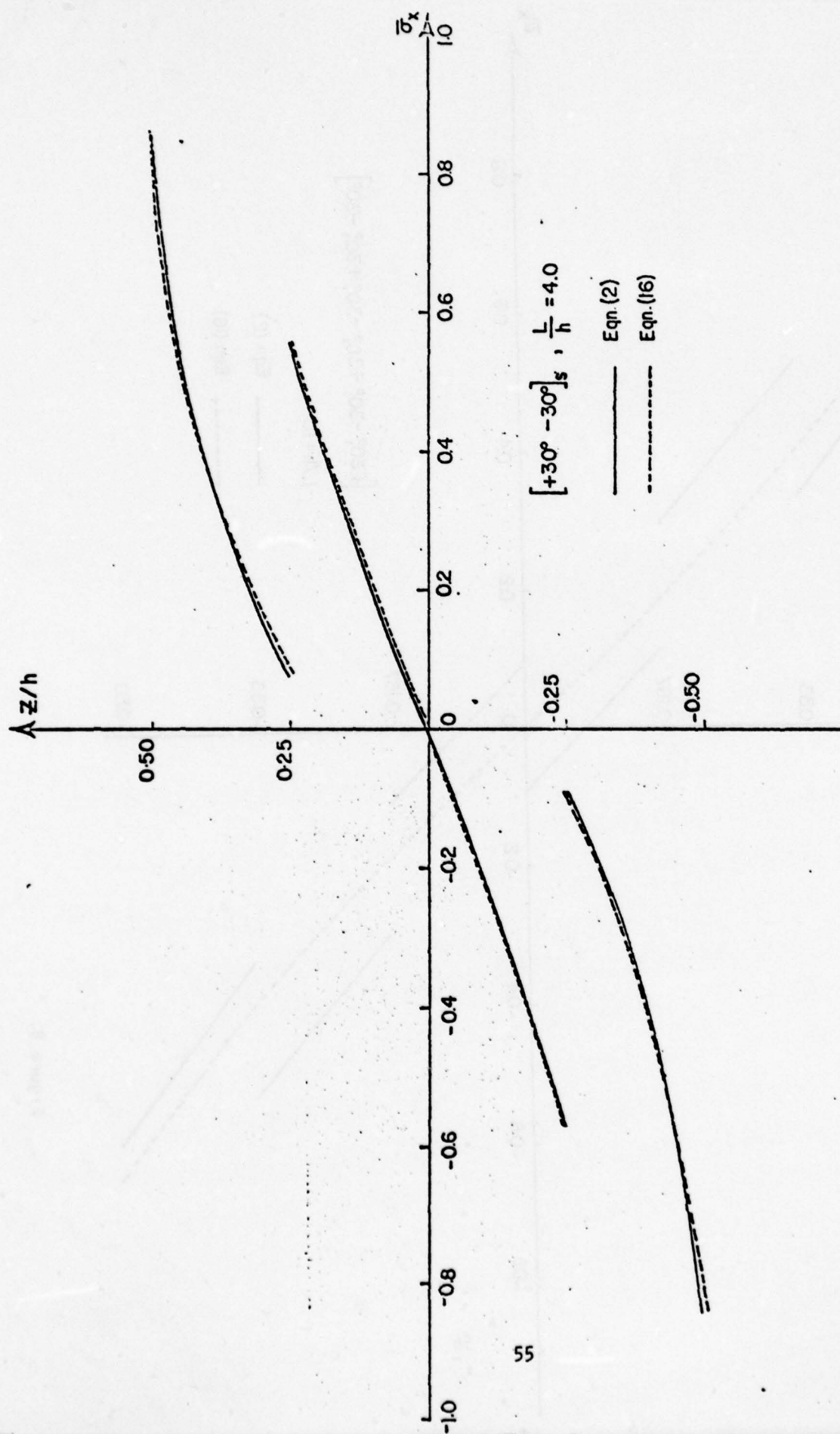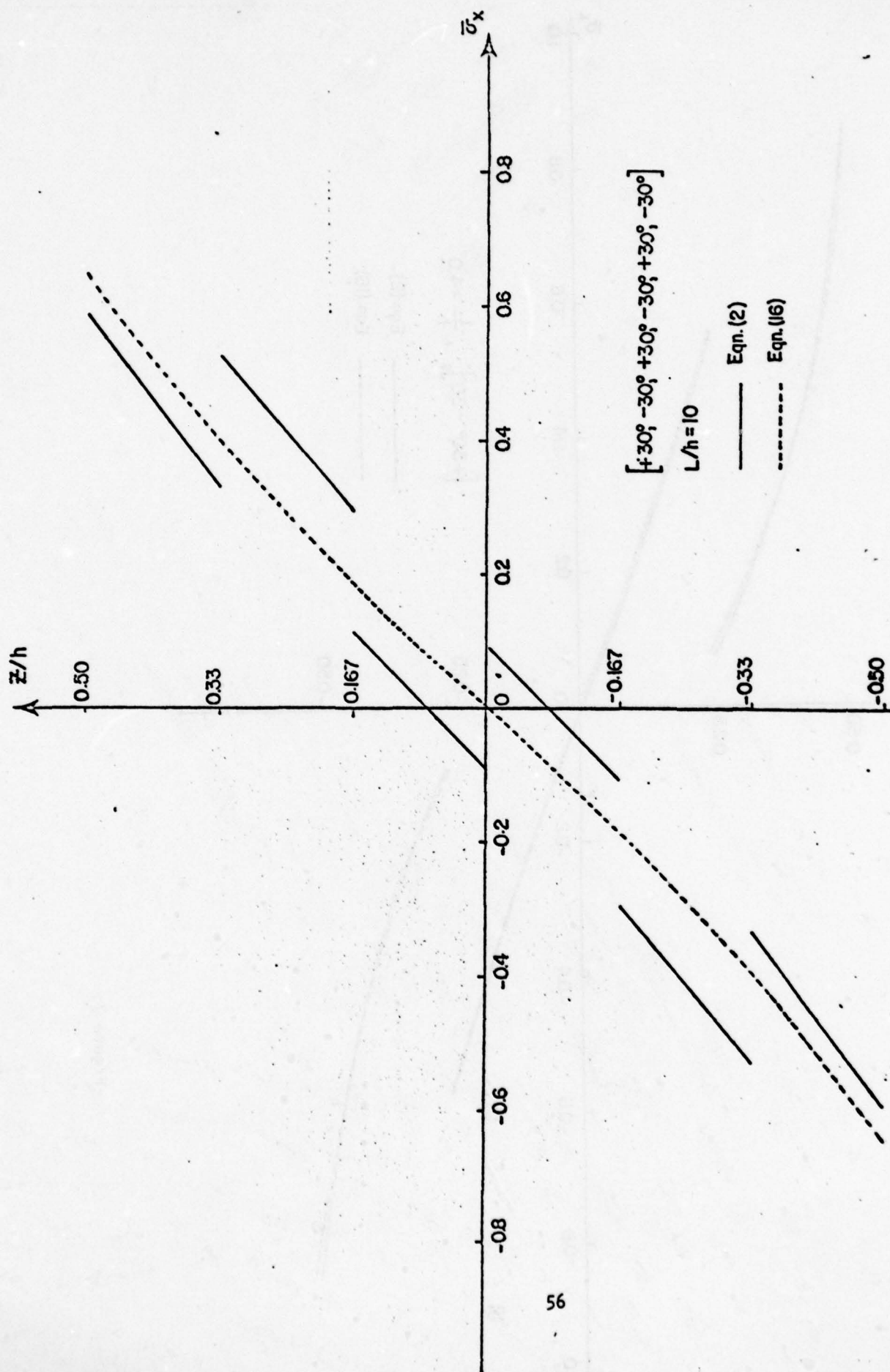
Figure 7.

Figure 8.

Chapter 3

STRESS SOLUTION DETERMINATION FOR
HIGH ORDER PLATE THEORY

K. H. Lo, R. M. Christensen and E. M. Wu

57

ABSTRACT

The high order theory of plate deformation developed in References [1] and [2] is further examined herein. Specifically, stress solutions are given and evaluated against exact elasticity solutions under stringent short wave length load conditions. By the first method the stresses are evaluated directly from the resulting displacement solutions. In a more refined procedure, the transverse shear stresses and the transverse normal stress are evaluated by an alternate equilibrium method. The latter procedure is shown to be more accurate than the former.

INTRODUCTION

It has long been recognized that classical plate theory must be modified to treat certain high order effects. The first comprehensive generalization of the classical theory was that given by Reissner [3]. Since Reissner's work, there have been a great many further generalizations beyond the classical theory assumptions, with perhaps the highest order theory to date being that given by Lo, Christensen and Wu [1] and [2]. Preliminary steps were taken in References [1] and [2] to assess the accuracy of the theory. In this paper this important subject is examined in greater detail.

The theory developed in References [1] and [2] is based upon an assumed displacement field of the type

$$u = u^\circ(x,y) + z\psi_x(x,y) + z^2\zeta_x(x,y) + z^3\phi_x(x,y)$$
$$v = v^\circ(x,y) + z\psi_y(x,y) + z^2\zeta_y(x,y) + z^3\phi_y(x,y) \qquad (1)$$
$$w = w^\circ(x,y) + z\psi_z(x,y) + z^2\zeta_z(x,y)$$

58

where u and v are the in-plane displacement components, w the out of plane or transverse components, z the normal coordinate, and the remaining functions in (1) depend upon the in-plane coordinate x and y. The governing theory, based upon the principle of stationary potential energy, resulted in eleven second order partial differential equations to determine the eleven functions in (1). It appears that an approach of this type is the logical way to proceed if one wishes to determine only the displacements. It is less clear that this approach is the most expeditious method if one seeks to determine stresses. Now the comparisons with exact elasticity results given in References [1] and [2] were only for the in-plane stress components, the transverse shear stresses and the transverse normal stress were not evaluated. Therefore the more complete stress information to be given here will help to answer the question of the general accuracy of the theory. Before proceeding with this however, it is useful to consider the three theoretical approaches to plate and shell development, and some advantages and disadvantages of each.

The first and most obvious approach to deriving an approximate plate theory utilizes assumptions upon the forms of displacements, as in (1). The governing differential equations could then be derived either by a direct method as in the case of classical plate theory, or by the use of the principle of stationary potential energy as in Reference [1]. Equilibrium is violated by this approach, that is to say, the equilibrium equations are only approximately satisfied through weighted averages. The second possible approach is the direct reversal of that just described. Stress expansions in z are assumed and the

59

governing differential equations are derived either by a direct approach or by the use of the complementary energy principle. Typical examples of this approach include the work of Reference [4]. In this method the equilibrium equations are satisfied, the stress strain relations are satisfied, but the compatibility of displacements is violated. In the third approach, assumptions are made upon both the stress states and the displacement forms where by both equilibrium and compatibility conditions are satisfied. However the stress strain relations are violated. Reissner's plate theory is the most common form of this type, Reference [3].

It is the stress state which usually is the item of interest in most problems. Accordingly it might seem to be most rational to use either of the latter two stress type theories, but not the theory which depends exclusively upon displacement assumptions. However, such reasoning involves one serious problem, namely it would eliminate the extension of the theory to model laminate behavior. This consequence is because of the fact that in laminates the in-plane stress components are discontinuous and it becomes as exceedingly complex matter to construct a high order theory which must inherently account for discontinuous stresses. However, even in laminates the displacements, of course, are continuous, and since a major impetus in constructing new high order theories is for use with laminates, it is herein considered necessary to proceed with the displacement theory of Reference [1]. The displacement theory of Reference [1] in fact has been extended to model laminates by Lo, Christensen and Wu [2].

60

This status of affairs still leaves us with some uncertainty. Is the displacement type theory of References [1] and [2] the best means by which to deduce the stress state under conditions where high order effects are of importance? The doubt arises because the equilibrium conditions are violated by the theory wheras stresses possess a one to one correspondence to the equilibrium conditions. However, there is one possible means by which the accuracy of the stresses obtained by this displacement type theory can be improved. The possible procedure is as follows. Use the high order theory based upon (1) to deduce the in-plane stress components, σ_x, σ_y, and τ_{xy}. Then insert these stress solutions into the equilibrium equations and solve for the out of plane/transverse stress components τ_{yz}, τ_{zx} and σ_z by integration. This procedure clearly results in a stress solution which satisfies equilibrium exactly. The procedure is suggested by the classical theory approach, which does not directly provide a solution for the transverse stress components, and they have to be found by the method described above.

Thus, the stresses implicity in the high order displacement type theory of References [1] and [2] will be determined by two separate means. First the in-plane and transverse stresses will be found directly from the displacement solution through the use of the strain-displacement and stress strain relations. By the second method the in-plane stresses will be found by the method just described and they will then be used to determine the transverse stresses by integrating the equations of equilibrium. These two alternate methods of deducing stress will be compared and tested against exact elasticity

61

solutions. Both cases of homogeneous plates and laminates will be considered.

THEORETICAL CONSIDERATIONS

The assumed displacement fields are given by relations (1). The polynomial expansion for w is truncated at one order lower than the expansions for u and v such that the contributions to the transverse shear strains from u and v are of the same order in z as that from the terms in w. The strain-displacement relations of the linear theory of elasticity are

$$
\begin{aligned}
\varepsilon_x &= u^\circ{,}_x + z\psi_{x,x} + z^2\zeta_{x,x} + z^3\phi_{x,x} \\
\varepsilon_y &= v^\circ{,}_y + z\psi_{y,y} + z^2\zeta_{y,y} + z^3\phi_{y,y} \\
\varepsilon_z &= \psi_z + 2z\zeta_z
\end{aligned}
\tag{2}
$$

and

$$
\begin{aligned}
\gamma_{xy} &= \gamma_{xy}^\circ + z\Gamma_{xy} + z^2\beta_{xy} + z^3 K_{xy} \\
\gamma_{xz} &= \gamma_{xz}^\circ + z\Gamma_{xz} + z^2\beta_{xz} \\
\gamma_{yz} &= \gamma_{yz}^\circ + z\Gamma_{yz} + z^2\beta_{yz}
\end{aligned}
\tag{3}
$$

with

$$
\begin{aligned}
\gamma_{xy}^\circ &= u^\circ{,}_y + v^\circ{,}_x; \quad \gamma_{xz}^\circ = \psi_x + w^\circ{,}_x; \quad \gamma_{yz}^\circ = \psi_y + w^\circ{,}_y \\
\Gamma_{xy} &= \psi_{x,y} + \psi_{y,x}; \quad \Gamma_{xz} = 2\zeta_x + \psi_{z,x}; \quad \Gamma_{yz} = 2\zeta_y + \psi_{z,y} \\
\beta_{xy} &= \zeta_{x,y} + \zeta_{y,x}; \quad \beta_{xz} = 3\phi_x + \zeta_{z,x}; \quad \beta_{yz} = 3\phi_y + \zeta_{z,y} \\
K_{xy} &= \phi_{x,y} + \phi_{y,x}
\end{aligned}
\tag{4}
$$

62

The stress strain relations appropriate to an anisotropic material
are given by

$$
\begin{bmatrix} \sigma_x \\ \sigma_y \\ \sigma_z \\ \tau_{yz} \\ \tau_{xz} \\ \tau_{xy} \end{bmatrix} = \begin{bmatrix} C_{11} & C_{12} & C_{13} & C_{14} & C_{15} & C_{16} \\ & C_{22} & C_{23} & C_{24} & C_{25} & C_{26} \\ & & C_{33} & C_{34} & C_{35} & C_{36} \\ & & & C_{44} & C_{45} & C_{46} \\ & \text{Sym} & & & C_{55} & C_{56} \\ & & & & & C_{66} \end{bmatrix} \begin{bmatrix} \epsilon_x \\ \epsilon_y \\ \epsilon_z \\ \gamma_{yz} \\ \gamma_{xz} \\ \gamma_{xy} \end{bmatrix}
\tag{5}
$$

where C_{ij}, $i,j = 1, 2, \ldots, 6$ are the stiffness coefficients. The
derivation of the governing equations for this higher order plate
theory is given in Reference [1] for homogeneous isotropic plates,
and its extension to laminated plate conditions is given in
Reference [4]. The evaluation of the stresses will now be given by
the two methods mentioned in the introduction.

STRESS EVALUATION, HOMOGENEOUS PLATE

An infinite homogeneous isotropic plate is subjected to sinusoidal
loadings as in Reference [1]. The prescribed surface tranctions are

$$
\sigma_z(h/2) = q_o \sin\left(\frac{\pi x}{L}\right); \quad \sigma_z(-h/2) - 0
\tag{6}
$$

and

$$
\tau_{xz}(\pm h/2) = \tau_{yz}(\pm h/2) = 0
\tag{7}
$$

where h is the plate thickness.

63

The solutions to the plate problems are [1],

$$u = [A_o + zA_1 + z^2A_2 + z^3A_3] \cos\left(\frac{\pi x}{L}\right)$$

$$v = 0 \tag{8}$$

$$w = [C_1 + zC_2 + z^2C_3] \sin\left(\frac{\pi x}{L}\right)$$

where the constants A_o, A_1, A_2, A_3 and C_1, C_2, and C_3 are obtained by satisfaction of the governing differential equations and boundary conditions. From (3), (4) and (5) the transverse stress components appropriate to a homogeneous isotropic plate are

$$\sigma_z = \lambda(u^\circ{,}_x + v^\circ{,}_y) + (\lambda + 2\mu)\,\psi_z$$
$$+ z[\lambda(\psi_{x,x} + \psi_{y,y}) + 2(\lambda + 2\mu)\zeta_z] \tag{9}$$
$$+ z^2\lambda(\zeta_{x,x} + \zeta_{y,y}) + z^3\lambda(\phi_{x,x} + \phi_{y,y})$$

and

$$\tau_{xz} = \mu(\psi_x + w^\circ{,}_x) + z\mu(2\zeta_x + \psi_{z,x}) + z^2\mu(3\phi_x + \zeta_{z,x})$$
$$\tau_{yz} = \mu(\psi_y + w^\circ{,}_y) + z\mu(2\zeta_y + \psi_{z,y}) + z^2\mu(3\phi_y + \zeta_{z,y}) \tag{10}$$

Substituting (8) into (9) and (10) gives the transverse stress components for the infinite plate

$$\sigma_z = \left\{ -\lambda A_o \frac{\pi}{L} + (\lambda+2\mu)C_2 + z\left[-\lambda A_1 \frac{\pi}{L} + 2(\lambda+2\mu)C_3\right]\right.$$
$$\left. - z^2\lambda A_2 \frac{\pi}{L} - z^3\lambda A_3 \frac{\pi}{L}\right\} \sin\left(\frac{\pi x}{L}\right) \tag{11}$$

and

$$\tau_{xz} = \left\{\mu\left[A_1 + C_1 \frac{\pi}{L}\right] + z\mu\left[2A_2 + C_2 \frac{\pi}{L}\right] + z^2\mu\left[3A_3 + C_3 \frac{\pi}{L}\right]\right\}\cos\left(\frac{\pi x}{L}\right) \tag{12}$$
$$\tau_{yz} = 0$$

64

These stresses are of course those deduced directly from the theory, and they will be displayed graphically for particular values of h/L, i.e. the ratio of the thickness of the plate to the characteristic length of the loading pattern. First of all, however, these same stress components will be evaluated by the alternate method mentioned in the introduction.

The in-plane stress components for the problem under consideration are given in Reference [1]. These in-plane stresses are substituted into the equilibrium equations

$$\sigma_{ij,j} = 0 \tag{13}$$

to yield, after integration, the out of plane/transverse stress components:

$$\sigma_z = \left\{ \frac{q_o}{2} + \frac{1}{2}\left[z^2 - \frac{h^2}{4}\right]\left[(\lambda+2\mu)A_o \frac{\pi^3}{L^3} - \lambda C_2 \frac{\pi^2}{L^2}\right] \right.$$

$$+ \frac{1}{12}\left[z^4 - \frac{h^4}{16}\right](\lambda+2\mu)A_2 \frac{\pi^3}{L^3}$$

$$+ \frac{z}{2}\left[\frac{z^2}{3} - \frac{h^2}{4}\right]\left[(\lambda+2\mu)A_1 \frac{\pi^3}{L^3} - 2\lambda C_3 \frac{\pi^2}{L^2}\right]$$

$$+ \frac{z}{4}\left[\frac{z^4}{5} - \frac{h^4}{16}\right](\lambda+2\mu)A_3 \frac{\pi^3}{L^3} \right\} \sin\left(\frac{\pi x}{L}\right) \tag{14}$$

and

$$\tau_{xz} = \left\{ z\left[(\lambda+2\mu)A_o \frac{\pi^2}{L^2} - \lambda C_2 \frac{\pi}{L}\right] \right.$$

$$+ \frac{1}{2}\left[z^2 - \frac{h^2}{4}\right]\left[(\lambda+2\mu)A_1 \frac{\pi^2}{L^2} - 2\lambda C_3 \frac{\pi}{L}\right]$$

$$+ \frac{z^3}{3}(\lambda+2\mu)A_2 \frac{\pi^2}{L^2} + \frac{1}{4}\left[z^4 - \frac{h^4}{16}\right](\lambda+2\mu)A_3 \frac{\pi^2}{L^2} \right\} \cos\left(\frac{\pi x}{L}\right) \tag{15}$$

65

where the top and bottom surface traction conditions (6) and (7) have been used to evaluate the constants of integration.

The corresponding exact elasticity solution for this problem is given in Reference [5], among many other sources. Before comparing the two alternate means of deriving the stresses, first the corresponding results for a particular laminated plate will be stated.

LAMINATED PLATE

The laminate to be considered is that of symmetric cross-ply geometry with each lamina being orthotropic. Using relations (5), (8), and (13), the transverse stress components are found to be

$$
\tau_{xz}^{(k)} = \left\{ -z \left[-c_{11}^{(k)} A_o \frac{\pi^2}{L^2} + c_{13}^{(k)} c_2 \frac{\pi}{L} \right] - \frac{z^2}{2} \left[-c_{11}^{(k)} A_1 \frac{\pi^2}{L^2} + 2c_{13} c_3 \frac{\pi}{L} \right] \right.
$$
$$
\left. + \frac{z^3}{3} \left[c_{11}^{(k)} A_2 \frac{\pi^2}{L^2} \right] + \frac{z^4}{4} \left[c_{11}^{(k)} A_3 \frac{\pi^2}{L^2} \right] \right\} \cos \left(\frac{\pi x}{L} \right)
$$
$$
+ f^{(k)}(x) \tag{16}
$$

and

$$
\sigma_z^{(k)} = \left\{ \frac{z^2}{2} \left[c_{11}^{(k)} A_o \frac{\pi^3}{L^3} - c_{13}^{(k)} c_2 \frac{\pi^2}{L^2} \right] + \frac{z^3}{6} \left[c_{11}^{(k)} A_1 \frac{\pi^3}{L^3} \right. \right.
$$
$$
\left. - 2c_{13}^{(k)} c_3 \frac{\pi^2}{L^2} \right] + \frac{z^4}{12} c_{11}^{(k)} A_2 \frac{\pi^3}{L^3}
$$
$$
\left. + \frac{z^5}{20} c_{11}^{(k)} A_3 \frac{\pi^3}{L^3} \right\} \sin \left(\frac{\pi x}{L} \right) - z f^{(k)}(x),_x
$$
$$
+ g^{(k)}(x) \tag{17}
$$

66

where the index k refers to the kth layer and where $f^{(k)}(x)$ and $g^{(k)}(x)$ are determined from the boundary and continuity conditions. These transverse stresses are those found by the method involved in using the in-plane stresses in the equations of equilibrium which are then integrated to find the three remaining transverse stress components.

Further consideration will be limited to the case of a three layer laminate arranged with the fiber directions designated by [0°/90°/0°] and with the laminae having equal thickness of h/3. The following expressions are obtained for $f^{(k)}(x)$ and $g^k(x)$.

$$f^{(1)}(x) = \left\{ \frac{h}{2}\left[-C_{11}^{(1)}A_o \frac{\pi^2}{L^2} + C_{13}^{(1)}C_2 \frac{\pi}{L} \right] + \frac{h^2}{8}\left[-C_{11}^{(1)}A_1 \frac{\pi^2}{L^2} + 2C_{13}^{(1)}C_3 \frac{\pi}{L} \right] \right.$$
$$\left. - \frac{h^3}{24}C_{11}^{(1)}A_2 \frac{\pi^2}{L^2} - \frac{h^4}{64}C_{11}^{(1)}A_3 \frac{\pi^2}{L^2} \right\} \cos\left(\frac{\pi x}{L}\right) \qquad (18)$$

$$f^{(2)}(x) = f^{(1)}(x) + \left\{ \frac{h}{6}\left[-[C_{11}^{(2)}-C_{11}^{(1)}]A_o \frac{\pi^2}{L^2} + [C_{13}^{(2)} - C_{13}^{(1)}]C_2 \frac{\pi}{L} \right] \right.$$

$$+ \frac{h^2}{72}\left[-[C_{11}^{(2)} - C_{11}^{(1)}]A_1 \frac{\pi^2}{L^2} + 2[C_{13}^{(2)} - C_{13}^{(1)}]C_3 \frac{\pi}{L} \right]$$

$$\left. - \frac{h^3}{648}[C_{11}^{(2)} - C_{11}^{(1)}]A_2 \frac{\pi^2}{L^2} - \frac{h^4}{5184}[C_{11}^{(2)} - C_{11}^{(1)}]A_3 \frac{\pi^2}{L^2} \right\} \cos\left(\frac{\pi x}{L}\right)$$
$$(19)$$

$$f^{(3)}(x) = \left\{ -\frac{h}{2}[-C_{11}^{(1)}A_o \frac{\pi^2}{L^2} + C_{13}^{(1)}C_2 \frac{\pi}{L}] + \frac{h^2}{8}[-C_{11}^{(1)}A_1 \frac{\pi^2}{L^2} \right.$$

$$\left. + 2C_{13}^{(1)}C_3 \frac{\pi}{L}] + \frac{h^3}{24}C_{11}^{(1)}A_2 \frac{\pi^2}{L^2} - \frac{h^4}{64}C_{11}^{(1)}A_3 \frac{\pi^2}{L^2} \right\} \cos\left(\frac{\pi x}{L}\right) \qquad (20)$$

67

$$g^{(1)}(x) = q_0 \sin\left(\frac{\pi x}{L}\right) + \frac{h}{L} f^{(1)}_{,x}(x) - \left\{\frac{h^2}{8}\left[C_{11}^{(1)}A_0 \frac{\pi^3}{L^3}\right.\right.$$

$$\left. - C_{13}^{(1)}C_2 \frac{\pi^2}{L^2}\right] + \frac{h^3}{48}\left[C_{11}^{(1)}A_1 \frac{\pi^3}{L^3} - 2C_{13}^{(1)}C_3 \frac{\pi^2}{L^2}\right]$$

$$\left. + \frac{h^4}{192} C_{11}^{(1)}A_2 \frac{\pi^3}{L^3} + \frac{h^5}{640} C_{11}^{(1)}A_3 \frac{\pi^3}{L^3}\right\} \sin\left(\frac{\pi x}{L}\right) \qquad (21)$$

$$g^{(2)}(x) = \frac{h}{6}\left[f^{(2)}_{,x}(x) - f^{(1)}_{,x}(x)\right] + g^{(1)}(x)$$

$$+ \left\{\frac{h^2}{72}\left[(C_{11}^{(1)}-C_{11}^{(2)})A_0 \frac{\pi^3}{L^3} - (C_{13}^{(1)}-C_{13}^{(2)})C_2 \frac{\pi^2}{L^2}\right]\right.$$

$$+ \frac{h^3}{1296}\left[C_{11}^{(1)}-C_{11}^{(2)})A_1 \frac{\pi^3}{L^3} - 2(C_{13}^{(1)}-C_{13}^{(2)})C_3 \frac{\pi^2}{L^2}\right]$$

$$+ \frac{h^4}{15552} (C_{11}^{(1)}-C_{11}^{(2)})A_2 \frac{\pi^3}{L^3} + \frac{h^5}{155520} (C_{11}^{(1)}-C_{11}^{(2)})A_3 \frac{\pi^3}{L^3}$$

$$\left.\right\} \sin\left(\frac{\pi x}{L}\right) \qquad (22)$$

and

$$g^{(3)}(x) = -\frac{h}{2} f^{(3)}_{,x}(x) - \left\{\frac{h^2}{8}\left[C_{11}^{(1)}A_0 \frac{\pi^3}{L^3} - C_{13}^{(1)}C_2 \frac{\pi^2}{L^2}\right]\right.$$

$$- \frac{h^3}{48}\left[C_{11}^{(1)}A_1 \frac{\pi^3}{L^3} - 2C_{13}C_3^{(1)} \frac{\pi^2}{L^2}\right] + \frac{h^4}{192} C_{11}^{(1)}A_2 \frac{\pi^3}{L^3}$$

$$\left. - \frac{h^5}{640} C_{11}^{(1)}A_3 \frac{\pi^3}{L^3}\right\} \sin\left(\frac{\pi x}{L}\right) \qquad (23)$$

68

where the subscripts 1, 2, and 3 refer to the 0°, 90°, and 0° layers, respectively.

The stress distributions will be displayed for lamina of the following properties which are typical of high modulus graphite/epoxy composites

$$E_2 = 25 \times 10^6 \text{ psi}; \; E_T = 10^6 \text{ psi}$$

$$G_{LT} = 0.5 \times 10^6 \text{ psi}; \; G_{TT} = 0.2 \times 10^6 \text{ psi} \quad (24)$$

$$\nu_{LT} = \nu_{TT} = 0.25$$

where L and T refer to the properties alone and transverse to the fiber directions, respectively, and ν_{LT} is the Poisson's ratio measuring transverse strain under normal stress parallel to the fibers.

DISCUSSION

The transverse normal stress and transverse shear stress for the homogeneous isotropic plate case are given in Figures 1-3. The difference in these figures is due to the variation in the ratio of h/L, i.e. the ratio of thickness to half wave length of the sinusoidal load. In Figure 1, for h/L = 1/4, the normal stresses calculated by the two different means are compared with the exact solutions. For this small value of h/L, the transverse shear stresses calculated by the two methods are so close to the exact solutions as to make them look identically equal graphically. Clearly the transverse normal stresses found by the integration of the equations of equilibrium are far more accurate than those obtained directly from the displacement

69

solution through the strain displacement and the stress strain relations. The results shown in these figures reveal that the transverse stresses found by equilibrium equation integration to be more accurate than those found directly from the displacement solution, with these results being under stringent short wave length load conditions. As discussed in Reference [1] the maximum ratio of h/L for which the theory has reasonable validity is about h/L = 1 and the results shown here collaborate this conclusion.

It is of interest to note from Figures 1-3 that the transverse stresses obtained directly from the displacement solution violate the top and bottom traction conditions. An examination of the derivation in Reference [1] reveals this to be a consistent aspect of the method. Thus even though the tractions enter the theory as boundary conditions, this process actually occurs through an equilibrium weighting method, thus the theory does not provide exact satisfaction of these boundary conditions. Consider however, the alternate method of obtaining the transverse stresses from integrating the equilibrium equations utilizing the in-plane stresses found directly from the displacement solution. In this case the boundary tractions are automatically satisfied through the evaluation of the constants of integration. A similar situation exists in the case of laminated plates. Transverse stresses evaluated directly from the displacement solution would in general not be continuous across the interfaces between lamina, however the transverse stresses found by the equilibrium method proposed herein provide continuous stress with exact satisfaction of top and bottom surface conditions.

70

The results for a three layer laminate are shown in Figures 4 and 5, for the value of h/L = 1/4. The exact elasticity solution is taken from Pagano [6]. It is apparent that the case of the laminate provides much more strenuous conditions against which to test a plate theory than does homogeneous conditions. Nevertheless, as seen in these figures the equilibrium equation method of generating transverse stresses provides a reasonable approximation to the exact solution.

CONCLUSIONS

The present high order theory of plate deformation appears to provide reasonably accurate predictions of behavior under short wave length conditions. This conclusion is valid for both homogeneous plates and for laminates; also as shown by the results, laminates are much more demanding of high order effect representation than are homogeneous plates. In problems where displacements are the quantity of prime interest the present displacement type theory appears to provide a reasonable and high order effect solution. In problems where the stresses are the quantity sought it has been shown that the present theory still provides highly accurate stress information. It has been demonstrated that the best method for determining the stresses involves determining the in-plane stresses directly from the displacement solution and thence determining the transverse stresses through the integration of the equations of equilibrium, utilizing the in-plane solution therein. This method is of course applicable to a theory of any order not just the present high order theory. The success of

71

the method was virtually assured by the fact that it is the only possible procedure for use at the level of the classical theory assumptions.

REFERENCES

1. K. H. Lo, R. M. Christensen, and E. M. Wu – A High order Theory of Plate Deformation. Part I: Homogeneous Plates. To be published in Journal of Applied Mechanics.

2. K. H. Lo, R. M. Christensen, and E. M. Wu – A High Order Theory of Plate Deformation. Part II: Laminated Plates. To be published in Journal of Applied Mechanics.

3. E. Reissner – The Effect of Transverse Shear Deformation on the Bending of Elastic Plates. J. Applied Mechanics, Vol. 12, No. 2, Trans. ASME, Vol. 67, June 1945, pp. 69-77.

4. S. A. Ambartsumyan – Theory of Anisotropic Plates. Technomic Publishing Company, Inc., 1970.

5. R. W. Little – Elasticity. Prentice-Hall, Inc., 1973.

6. N. J. Pagano – Exact Solutions for Composite Laminates in Cylindrical Bending. J. Composite Materials, Vol. 3, 1969, pp. 398-411.

73

FIGURE CAPTIONS

Figure 1. Transverse normal stress distributions for a homogeneous isotropic plate at h/L = 0.25.

Figure 2. Transverse normal stress distributions for a homogeneous isotropic plate at h/L = 1.0.

Figure 3. Transverse shear stress distributions for a homogeneous isotropic plate at h/L = 1.0.

Figure 4. Transverse normal stress distributions for a [0°, 90°, 0°] laminate at h/L = 0.25.

Figure 5. Transverse shear stress distributions for a [0°, 90°, 0°] laminate at h/L = 0.25.

74

Figure 1.

$h/L = 0.25$

EXACT ELASTICITY SOLUTION AND
EQUILIBRIUM EQUATION METHOD

DIRECT METHOD

75

Figure 2.

EXACT ELASTICITY SOLUTION
EQUILIBRIUM EQUATION METHOD
DIRECT METHOD

$h/L = 1.0$

Figure 3.

77

z/h

0.5
0.4
0.3
0.2
0.1
0
-0.1
-0.2
-0.3
-0.4
-0.5

0.5   1.0 σ_z/q_0

$[0°,90°,0°]$, h/L = 0.25

EXACT ELASTICITY SOLUTION

EQUILIBRIUM EQUATION METHOD

CLASSICAL PLATE THEORY

Figure 4.

78

$[0°, 90°, 0°]$, $h/L = 0.25$

EXACT ELASTICITY SOLUTION
EQUILIBRIUM EQUATION METHOD
CLASSICAL PLATE THEORY

Figure 5.

79
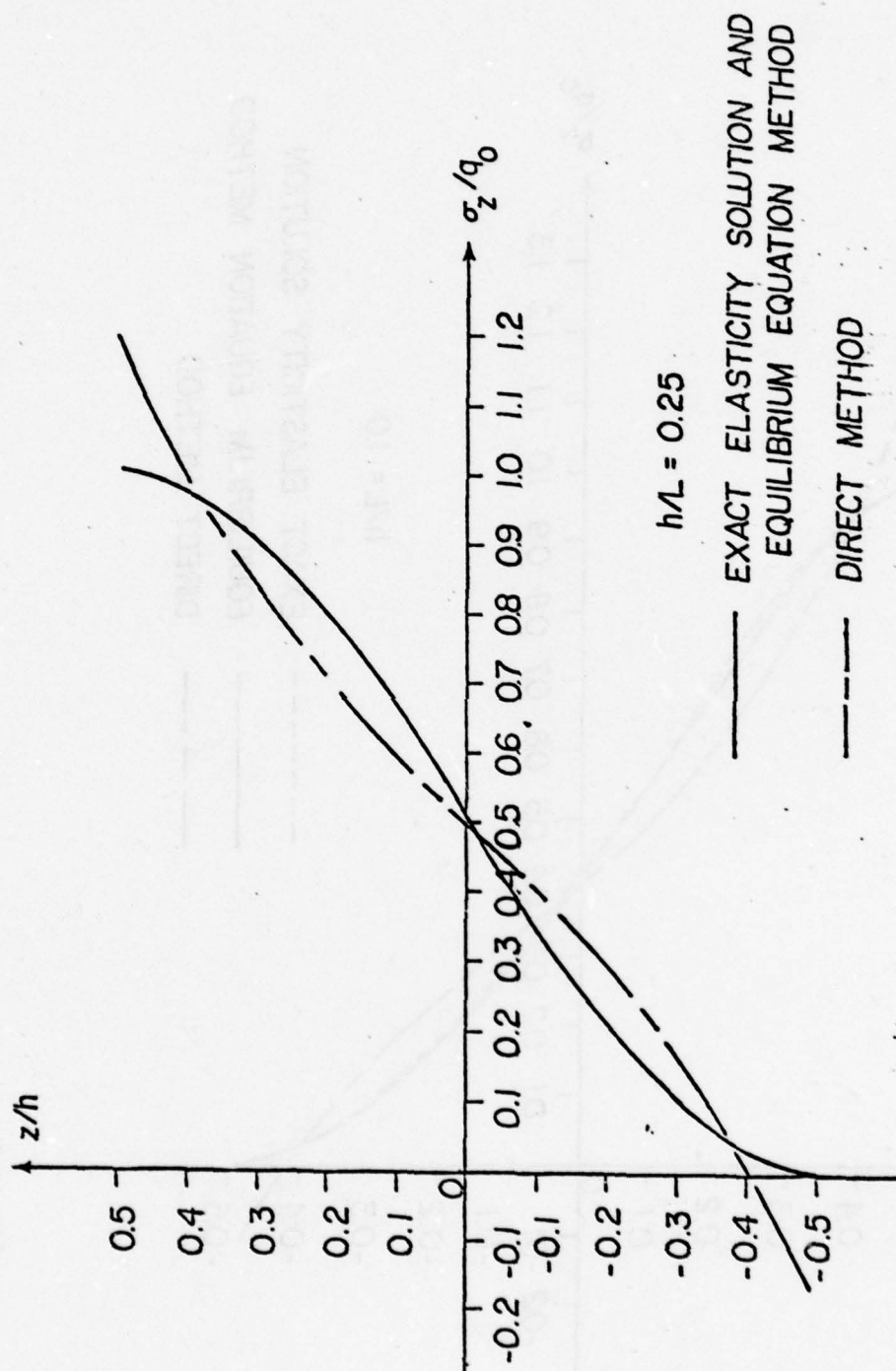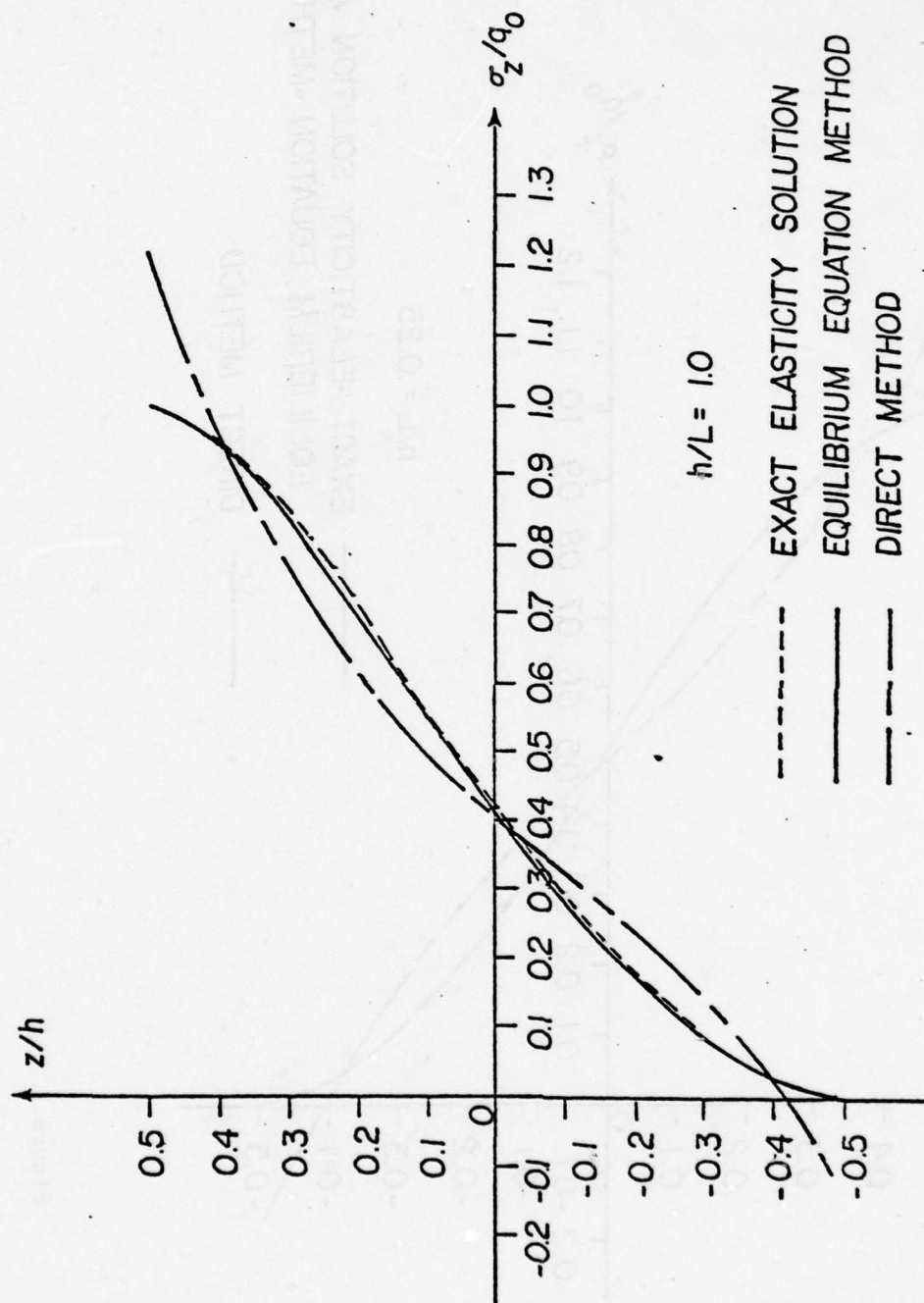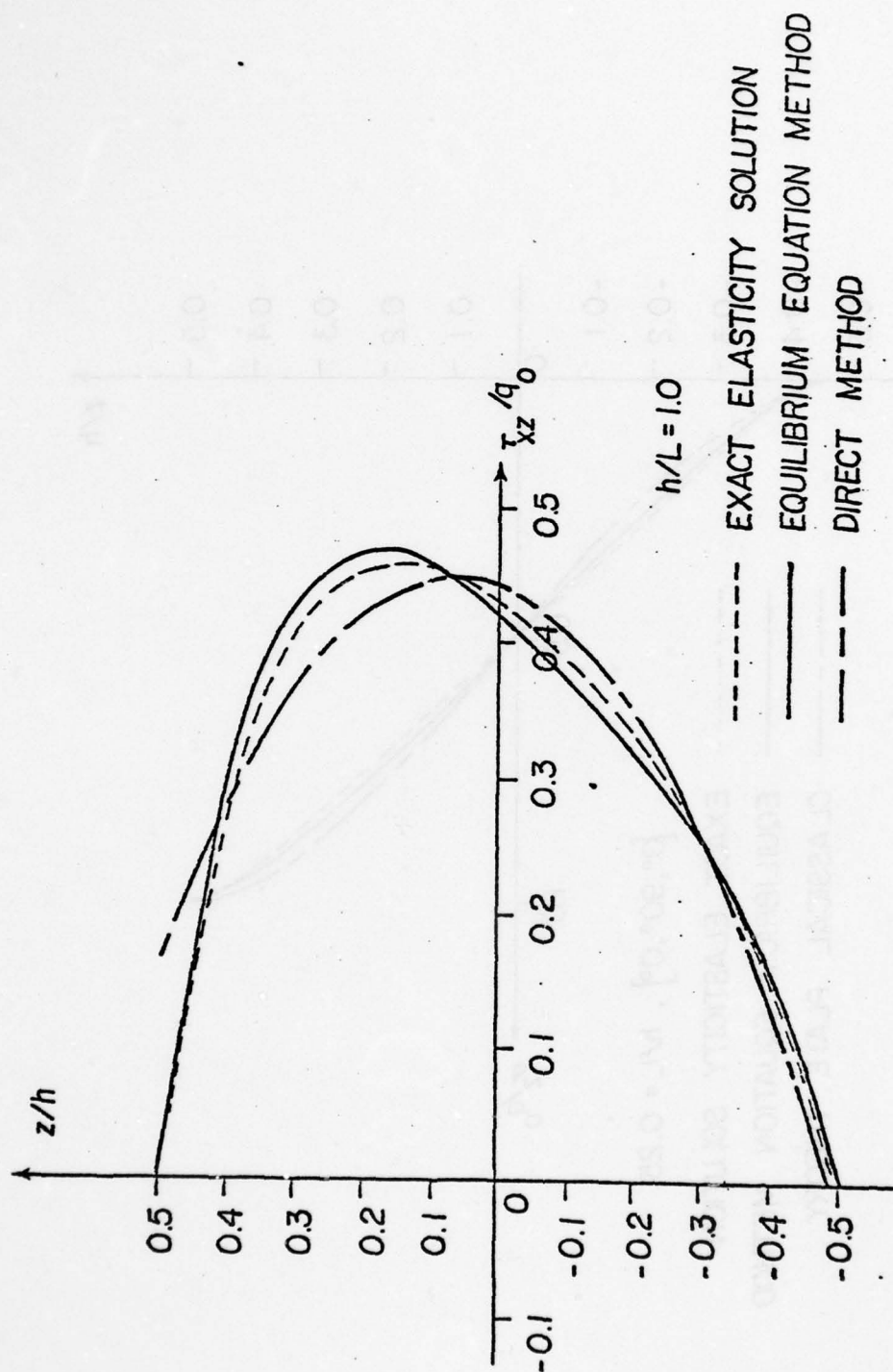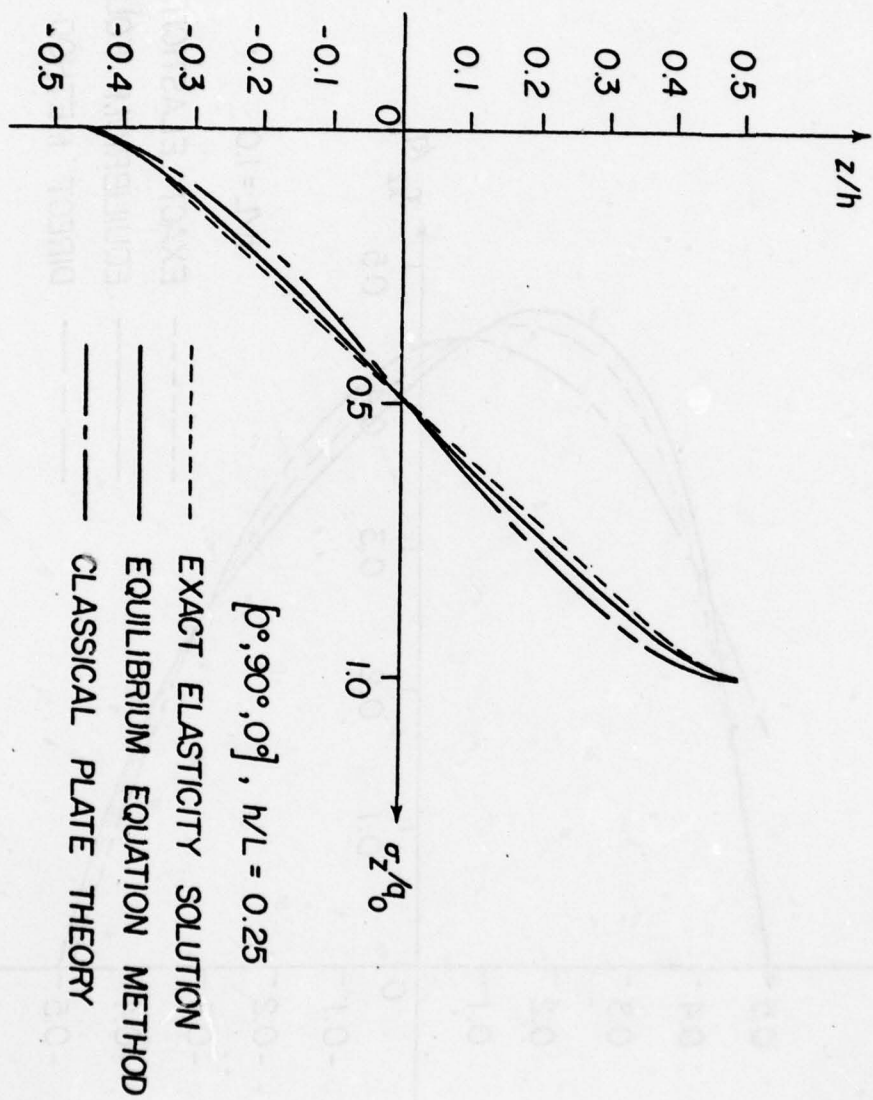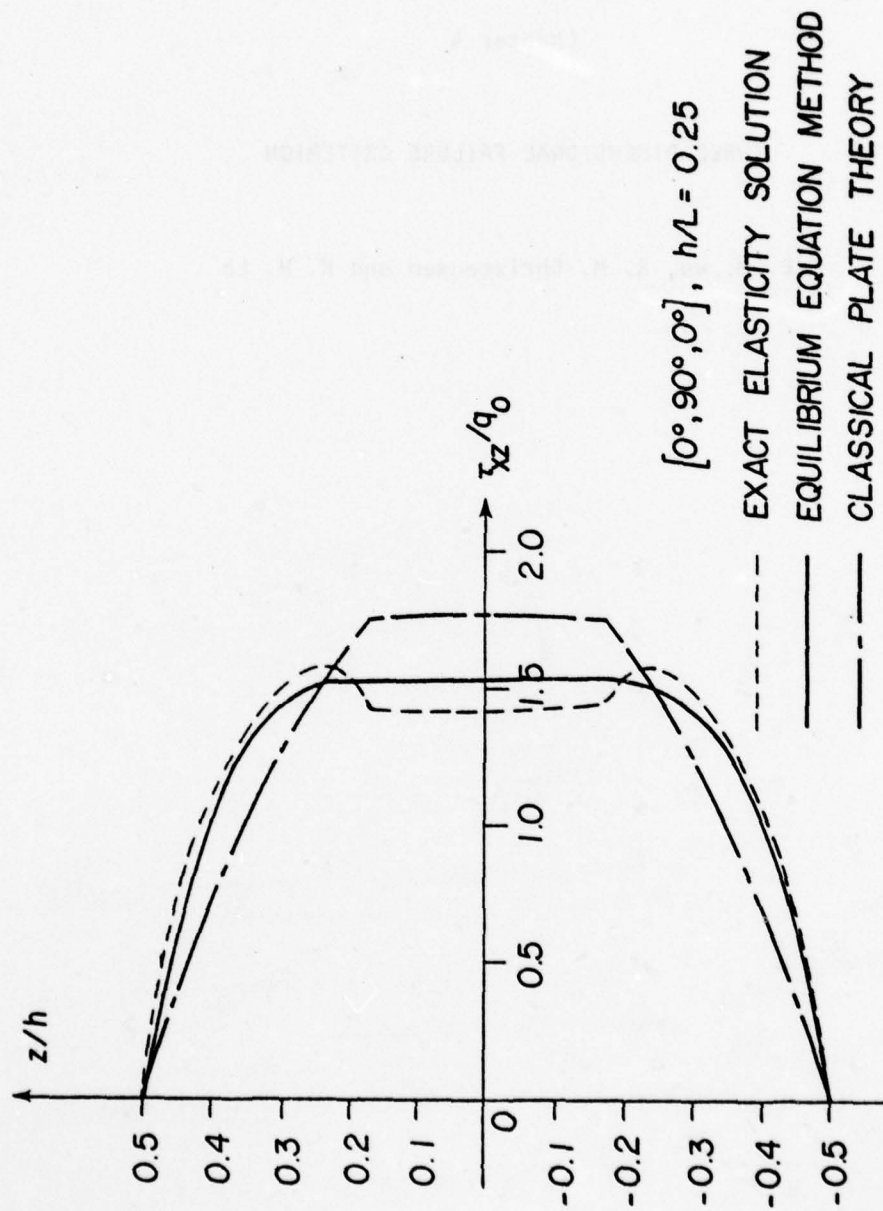
Chapter 4

THREE DIMENSIONAL FAILURE CRITERION

E. M. Wu, R. M. Christensen and K. H. Lo
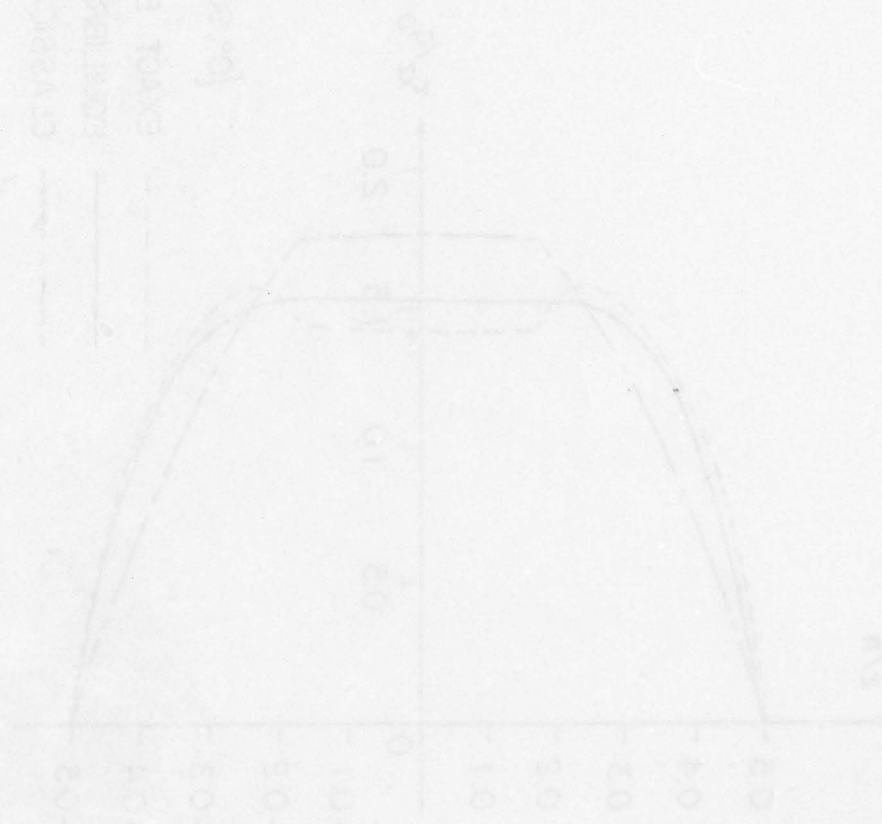
Strength of Thick Laminates

The strength of thick laminates can be cast in terms of the characterization of the criticality of three-dimensional stress states, which can lead to rupture. Due to the complexity of this characterization, the following simplified assumptions are required: 1) all combined loadings are proportional and monotonic thus precluding the effects of fatigue and loading path dependency, 2) the thick composite is planar laminated thus precluding 3-D woven structures. Within these constraints, significant flexibility is retained, e.g. the lamination sequence and angle can be arbitrarily varied utilizing a single set of basic data, or if basic data are available for several generically different laminae, thick hybrid composite laminate strengths can also be estimated.

The flexibility of this characterization lies in the inclusion of three-dimensional stresses in the tensor polynomial failure criterion for the lamina. Since the coefficinets of the tensor polynomial failure criterion obey tensor transformation laws, computational methods for predicting the strength of thick laminae of any layup can be established.

The principle steps of this characterization are:

1) Evaluation of the 3-D failure criterion for a unidirectional lamina,

2) Establishment of the transformational properties of the strength coefficients,

3) 3-D analysis of thick laminated structure.

These steps are illustrated in Figures 1a, b, c respectively. The last step has already been addressed in Chapters 1, 2, and 3. The first and

81

second steps will now be examined. In Step 1 (Figure 1a) we seek the strength response of the lamina (along its principal directions) which can be expressed in terms of the tensor failure polynomial criterion as [1]:

$$F_i \sigma_i + F_{ij} \sigma_i \sigma_j + \ldots = 1 \qquad i,j = 1,2,3,4,5,6 \qquad (1a)$$

The failure tensors which characterize the strength of the laminate can be written in matrix form, while accounting for orthotropy, as

$$F_i = \begin{bmatrix} F_1 \\ F_2 \\ F_3 \\ 0 \\ 0 \\ 0 \end{bmatrix} \qquad F_{ij} = \begin{bmatrix} F_{11} & F_{12} & F_{13} & 0 & 0 & 0 \\ & F_{22} & F_{23} & 0 & 0 & 0 \\ & & F_{33} & 0 & 0 & 0 \\ & & & F_{44} & 0 & 0 \\ & & & & F_{55} & 0 \\ & & & & & F_{66} \end{bmatrix} \qquad (1b)$$

It is seen from Equation (1b) that the failure tensors associated with the 3 axis (F_3, F_{13}, F_{23}, F_{33}, F_{44}, F_{55}) control the strength related to the stresses assocated with the 3 axis. These coefficients are not required if the laminate is thin but must be included if the laminate is thick. The remaining coefficinets are well known and they may be measured by a total of six independent experiments. It appears that measurement of the failure tensors, associated with the inclusion of the 3 axis requires six additional tests. However symmetry conditions will be explored to reduce the number of tests.

A unidirectional lamina (oriented as shown in Figure 1(a)) possesses the symmetry condition that properties associated with the X_2 are

interchangeable with properties associated with the X_3 axis. Thus, the following table of symmetry for the strength coefficients can be constructed.

Table I

Tensor Notation	Contracted Notation
$F_{22} = F_{33}$	$F_2 = F_3$
$F_{1122} = F_{1133}$	$F_{12} = F_{13}$
$F_{2222} = F_{3333}$	$F_{22} = F_{33}$
$F_{1313} = F_{1212}$	$F_{55} = F_{66}$

By virtue of these symmetries, we can assess the necessary experiments required to evaluate the coefficinets for a 3-D failure criterion. These experiments can be determined by evaluation of Equation (1a) following the procedure outlined by Wu in Reference [2]. By substitution of different stress states in Equation (1a), we can evaulate the coefficients of the strength tensors:

83

Evaluation of Component of Strength Tensor*	State of Stress Required

F_1 , F_{11}

(1)   (2)

F_2 , F_{22} , (F_3, F_{33})

(3)   (4)

F_{66} (F_{55})

(5)

F_{12} , (F_{13})

(6)

F_{23} (F_{32})

(7)

F_{44}

(8)
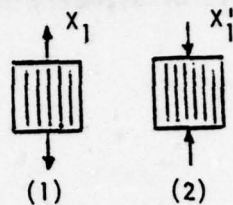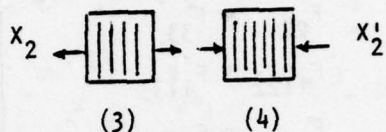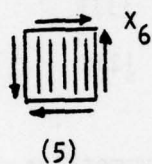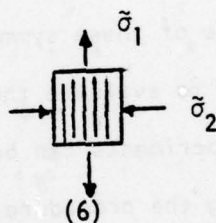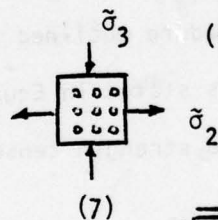
* Bracketed terms, by symmetry

Here, we adopt the same notation as in Reference [2] where X_i represents the uniaxial strength induced by the uniaxial stress σ_i and $\tilde{\sigma}_i$ are the biaxial strengths induced by combined stress conditions. The strength tensor is computatable from the strengths by solution of Eq. (1). The necessary relations are: for experiments No. 1, 2, 3, 4, 5, and 8,

$$\left. \begin{array}{l} F_i = \dfrac{1}{X_i} - \dfrac{1}{X_i{}'} \\[2em] F_{ij} = \dfrac{1}{X_i X_i{}'} \end{array} \right\} \begin{array}{l} \text{no sum} \\ i = 1,\ 2,\ 3,\ 4,\ 5,\ 6. \end{array} \qquad (2)$$

for experiments No. 6,

$$F_{12} = (1 - F_1\tilde{\sigma}_1 - F_2\tilde{\sigma}_2 - F_{11}\tilde{\sigma}_1{}^2 - F_{22}\tilde{\sigma}_2{}^2)\, \frac{1}{2\tilde{\sigma}_1\tilde{\sigma}_2} \qquad (3)$$

For experiment No. 7,

$$F_{23} = (1 - F_2\tilde{\sigma}_2 - F_3\tilde{\sigma}_3 - F_{22}\tilde{\sigma}_2{}^2 - F_{33}\tilde{\sigma}_3{}^2)\, \frac{1}{2\tilde{\sigma}_2\tilde{\sigma}_3} \qquad (4)$$

We note that tests No. (1) through (6) are those required for a two-dimensional failure criterion; the procedure for determining them has been thoroughly described in Reference [2]. In addition, we uncovered a rather surprising and convenient fact that a three-dimensional failure criterion (in 2nd-order form) only required two additional experiments i.e., tests No. 7 and No. 8. In fact, we note that experiemnts No. 7 and No. 8 are measuring the strength response of

85

essentially isotropic properties. Thus, a not unreasonable estimate of these strengths may be arrived at by degrading the corresponding resin matrix strengths by a suitable factor to reflect the stress concentration due to the presence of fibers. If such a comprise is deemed acceptable; no additional tests are required to extend a 2-D failure criterion to a 3-D failure criterion! Such is the remuneration for the tensor polynomial failure criterion formulation. In this program these coefficients are experimentally measured rather than estimated.

Experimental Measurements

The failure criteria outlined here are evaluated for a ultra-high stiffness graphite epoxy composite-GY 70 manufactured by Celanese Corporation with Fiberite 934 Resin. Samples for this program was fabricated by General Dynamics Cooperation, Convair Division.

The eight characteristic experiments described previously were carried out. The sample configurations of these tests are as follows.

Experiment No. 1 (longitudinal tensile test) was performed on parallel-edged samples with end-tabs of the configuration referred to as IITRI samples recommended by the Air Force Design Guide. End tabs were not tapered and were fully loaded by wedge grips over its entire length to eliminate peeling by tensile stress.

Experiment No. 2 (longitudinal compression) was performed on a sandwich specimen. The configuration is shown in Fig. 2a and b. This compression sample is similar to the honeycomb sandwich sample

86

suggested in the Air Force Design Guide (MIL-STD-401A) with the difference that low density rigid foam is used in lieu of the usual honeycomb for expediency of sample preparation. Test results are consistent with those produced by the honeycomb sandwich samples.

Experiment No. 3 (Transverse tension) samples were identical to experiment No. 1 with the exception that end tabs were not used.

Experiment No. 4 (Transverse compression) samples were identical to those used in experiment no. 2.

Experiment No. 5 (Longitudinal shear) was performed by a beam bending configuration as shown in Fig. 3a and 3b. This shear test was originally suggested by Messmer [3] in photoelasticity experiments and subsequently rediscovered by Losipescu [4] to test shear strength of isotropic metals. The salient features of this configuration are that:

i) The one dimensional nature of the configuration lends itself to analysis which is accurate to the beam theory level.

ii) In beam bending theory, longitudinal shear is proportional to the gradient of the bending moment; in this configuration the bending moment gradient is uniform over the length of the beam and the magnitude of the moment is zero at the center. Thus if failure is induced to occur at the center, the strength measurement reflects the pure shear strength. For the purpose of inducing shear failure at the center and for the purpose of converting the parabolic distribution of shear stress to uniform shear stress, Losipesu [4] introduced 90° notches to the sample. While this technique was reported to work satisfactorily for metals, it proved to be unsuccessful for

87

unidirectional lamina because machining of the 90° notch inevitably
induced cracking. We overcame this difficulty by introducing
bonding flanges to the composite web to form the shape of an I beam.
The flanges (top and bottom) are discontinuous at the center (see
Figure 4); since the moment is zero in the center with no normal stress
due to bending, no stress singularity is induced by the slit. At the
same time, shear failure can propagate through the slit. The absence
of singularity is valid to the level of the strength of material
analysis but probably not in the theory-of-elasticity level. However,
verification was carried out to the extent that literature values on
known composites (Scotch-ply-1002) were recovered by this test.
It appears this test might merit more extensive development under a
different scope. Suggested studies are finite element and photo-
elastic analysis and optimization of the flange material.

Test No. 6 involved internal pressurization and compression of a
thin-walled tube. The stress ratio induced was $B = \sigma_1/\sigma_2 = -10$.
Experimental details are as described in Reference (5).

Test No. 7 was similar to a constrained compression test
reported by T. C. Collings [5] and is schematically illustrated in
Figure 5. The sample is a 3/4-inch cube cut from a thick lamina. For
the measured Poisson ratio, $\nu_{23} = 0.62$, the stress ratios are

$$\frac{\sigma_2}{\sigma_3} = \frac{-1}{-0.62} .$$

Test No. 8 was performed in the same fixture as in Test No. 5
(the longitudinal shear test), the exception being that in this case the

88

fiber orientation is perpendicular to the web (See Figure 6). These samples are sliced from a 0.75"-thick laminate with a diamond circular cutter.

All of the above experiments were performed on an electro-hydraulic servo-controlled testing machine. Load is used as the feedback control and the loading function is constant loading rate to failure. Loading rates for each type of tests were adjusted (by trial) such that starting from no load, the time to fail was approximately 10 minutes. The experimental results are:

Test	Strength (ksi)		Range
1. Longitudinal Tension	$X_1 =$	$\begin{cases} 81.6 \text{ (1st Batch)} \\ 80.9 \text{ (2nd Batch)} \end{cases}$	55.5 - 101 60.9 - 98.6
2. Longitudinal Compression	$X_1' = 82.3$		69.3 - 91.2
3. Transverse Tension	$X_2 = 5.1$		4.2 - 5.6
4. Transverse Compression	$X_2' =$	$\begin{cases} 8.6 \text{ (1st Batch)} \\ 7.9 \text{ (2nd Batch)} \end{cases}$	8.1 - 9.0 7.3 - 8.4
5. Longitudinal Shear	$X_6 = 8.2$		7.9 - 8.5
6. Biaxial Strength 1, 2 plane	$\begin{cases} \tilde{\sigma}_1 = 92.4 \\ \tilde{\sigma}_2 = -9.2 \end{cases}$		
7. Biaxial Strength 2, 3 plane	$\begin{cases} \tilde{\sigma}_2 = -85.6 \\ \tilde{\sigma}_3 = -53 \end{cases}$ (1st Batch) $\begin{cases} \tilde{\sigma}_2 = -87.9 \\ \tilde{\sigma}_3 = -42.3 \end{cases}$ (2nd Batch)		
8. Transverse Shear	$X_4 = 4.5$		3.9 - 4.8

89

Two batches of samples were tested to assure consistency of material
and instrumentation reproducibility. Stress-strain relations were
recorded and are shown in Figures 7 to 11. In Figure 7, the individual
stress-strain curves for longitudinal tension are presented. In
Figure 8, these tests are statistically averaged; the curves shown
are the averaged stress-strain curve and the $\pm$ Due Standard deviation
of the stress-strain curves; "X" are the ultimate values for each
individual samples. In similar forms, Figures 9 and 10 depict results
of transverse compression tests. Figures 11a and 11b are respectively
the stress-strain components in the 2 and 3 directions for biaxial
compression.

Based on these measured strengths the strength tensor is computed
in accordance with equations 2, 3 and 4; together with the symmetry
conditions, we deduced the strength tensor for GY 70/934 to be:

$$
\left.
\begin{aligned}
F_1 &= 0.157 \times 10^{-3} \\
F_2 &= 74.8 \times 10^{-3} \\
F_3 &= (74.8 \times 10^{-3}) \\
F_4 &= (0) \\
F_5 &= (0) \\
F_6 &= (0)
\end{aligned}
\right\} \frac{1}{\text{ksi}}
\qquad
\left.
\begin{aligned}
F_{11} &= 0.150 \times 10^{-3} \\
F_{22} &= 23.8 \times 10^{-3} \\
F_{33} &= (23.8 \times 10^{-3}) \\
F_{12} &= 0.954 \times 10^{-3} \\
F_{13} &= (0.954 \times 10^{-3}) \\
F_{23} &= -0.027
\end{aligned}
\right\} \frac{1}{\text{ksi}^2}
$$

The bracketed values are inferred from symmetry conditions.

Discussion and Conclusion

With these strength tensor components, we have a full characterization
of the 3-D strength of the GY 70/934 composite. This 3-D failure criterion

90
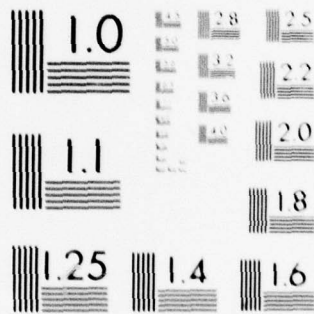
may be used to assess the criticality of a three-dimensional state of stress either computed from 3-dimensional analysis or the aforerepresented high-order plate analysis. Furthermore we note that biaxial compressive stress tends to increase the strength of the composite. For example both the biaxial tests No. 6 and 7 produced strength greater than the uniaxial strength X_1 and X_2' respectively. This is reflected in positiveness of the coefficient of strength tensor F_{12}, F_{13}, F_{23}. Physically this suggests that the composite test is probably microflaw sensitive in the transverse direction; application of transverse compression tends to retard flaw growth and lead to a strength increase in the longitudinal direction. This may be the reason for the large range in strength variability measured. Constraints in the program preclude further in-depth experimental measurement. Another effort has been initiated to check the experimental technique and provide further measurements. Nevertheless, the methodology and analysis remain well founded and may be applied with confidence.

References

1. E. M. Wu and S. W. Tsai, "A General Theory of Strength of Anisotropic Materials", Journal of Composite Materials, Vol. 5, p. 58.

2. Wu, E. M. "Phenomenological Anisotropic Failure Criterion" in Composite Materials, Vol. 2 (editor Sendeckyj) Series Editors Broutman and Krock. Academic Press 1974.

3. G. K. Messmer, "Spannungsoptik", Verlag von Julius Springer, Berlin 1939, p. 179.

4. Losipescu, N., "New Accurate Procedures for Simple Shear Testing of Metals", Journal of Materials, Vol. 2, No. 3, p. 537-566.

5. Wu, E. M., "Optimal Experimental Measurements of Anisotropic Failure Tensors", Journal of Composite Materials, Vol. 6, p. 472-489.

6. Collings, T. C., "Transverse Compress Behaivor of Unidirectional Carbon Fiber Reinforced Plastics", Composites, May 1974.

FIGURE CAPTIONS

Figure 1:   Composite Laminates

Figure 2:   Compression Sample Configuration (Test No. 2 and 4)

Figure 3:   Shear Fixture Configuration (Test No. 5)

Figure 4:   Shear Sample Configuration (Test No. 5)

Figure 5:   Biaxial Compression Configuration (Test No. 7)

Figure 6:   Shear Test Configuration (Test No. 8)

Figure 7:   Individual Stress-Strain Curves of Longitudinal Tension
              Tests of GY-70/934 (1 ksi = 0.145 MPa)

Figure 8:   Averaged Stress-Strain Curves of Longitudinal Tests of
              GY-70/934 (1 ksi = 0.145 MPa)

Figure 9:   Individual Stress-Strain Curves for Transverse Compression
              Tests of GY-70/934 (1 ksi = 0.145 MPa)

Figure 10:   Average Stress-Strain Curves of Transverse Compression
              Tests of GY-70/934 (1 ksi = 0.145 MPa)

Figure 11a: Individual σ_2 vs ϵ_3 Curves for Biaxial Compression in
              2-3 plane for GY-70/934 (1 ksi = 0.145 MPa)

Figure 11b: Individual σ_3 vs ϵ_3 Curves for Biaxial Compression in
              2-3 Plane for GY-70/934 (1 ksi = 0.145 MPa)

Figure 1. Composite Laminates.

Specimen

Alumina
End Caps

Rigid Foam
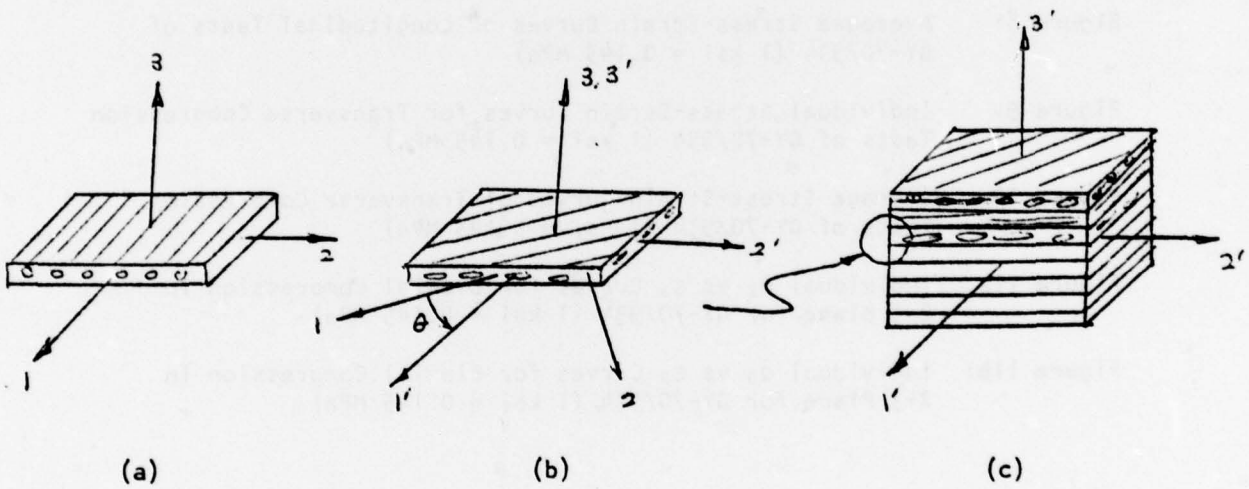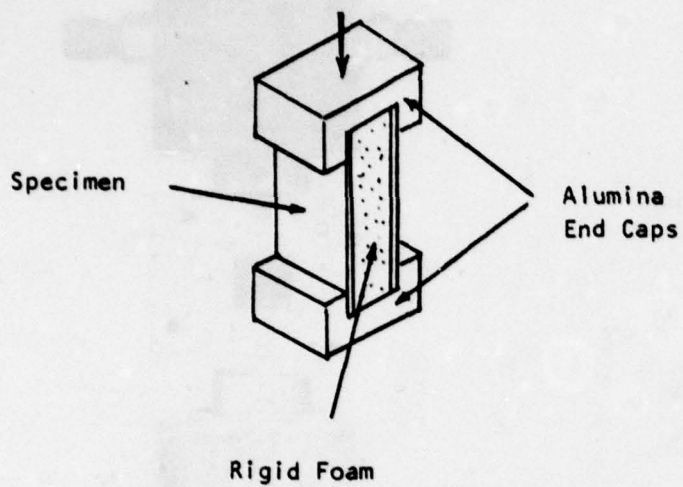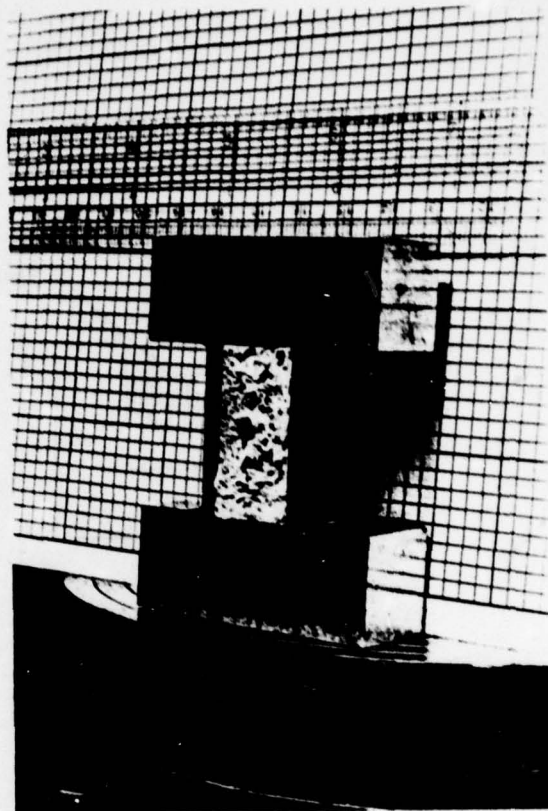
(a)   (b)

Figure 2.   Compression Sample Configuration (Test No. 2 and 4).
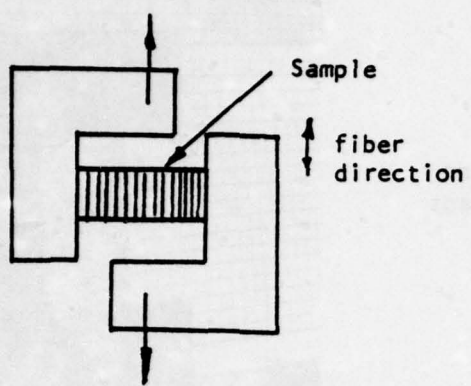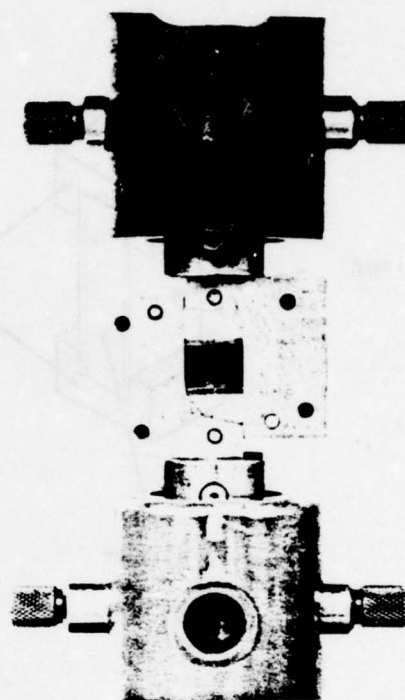
(a)   (b)

Figure 3. Shear Fixture Configuration (Test No. 5).

(a)

(b)

Figure 4. Shear Sample Configuration (Test No. 5).

97

Figure 5. Biaxial Compression Configuration (Test No. 7).

Figure 6. Shear Test Configuration (Test No. 8).

Figure 7. Individual Stress-Strain Curves of Longitudinal Tension Tests of GY-70/934 (1 ksi = 0.145 MPa).

100

STRAIN

LTEN1368 GD GY70 4 PLY .01 CM/MIN   (MPA)

AVERAGE CURVE..95 LIMITS,AND FAILURE POINTS FOR   9 SPECIMENS

THE AVERAGE VALUE AND COEFFICIENT OF VARIATION FOR
MAX. STRESS   5.580E+02 1.589E-01   AREA TO .25E   1.129E+02 4.491E+00
MAX. STRAIN   1.910E-03 1.490E-01   AREA TO MAX. STRESS 1.270E+02 4.897E+00
STRESS AT 0.00050   1.413E+02 3.837E-02   AREA TO RUPTURE STRESS 1.413E+02 5.423E+00
STRESS AT 0.00100   2.865E+02 3.602E-02   AREA TO RUPTURE STRESS
STRESS AT 0.00200   4.571E+02 5.879E-01   AREA TO RUPTURE STRESS
RUPT. STRESS   5.580E+02 1.589E-01
RUPT. STRAIN   1.910E-03 1.490E-01

Figure 8.   Averaged Stress-Strain Curves of Longitudinal Tests of GY-70/934
            (1 ksi = 0.145 MPa).

101

Figure 9. Individual Stress-Strain Curves for Transverse Compression Tests of GY-70/934 (1 ksi = 0.145 MPa).

102

STRESS (MPA)

70

60

50

40

30

20

10

0   .002 .004 .006 .008 .010 .012 .014 .016 .018 .020

STRAIN

LCOM1385   GY70/934 90 DEG   (MPA)

AVERAGE CURVE..95 LIMITS,AND FAILURE POINTS FOR 3 SPECIMENS

THE AVERAGE VALUE AND COEFFICIENT OF VARIATION FOR

MAX. STRESS	5.443E+01	6.252E-02	AREA TO .25E	1.370E+01 1.542E+00
MAX. STRAIN	1.432E-02	1.130E-01	AREA TO MAX. STRESS	1.526E+01 1.812E+00
STRESS AT 0.00050	3.473E+00	1.461E-01	AREA TO RUPTURE STRESS	1.704E+01 1.902E+00
STRESS AT 0.00100	6.786E+00	1.613E-01	AREA TO RUPTURE STRESS	
STRESS AT 0.00200	1.370E+01	1.126E-01	AREA TO RUPTURE STRESS	
RUPT. STRESS	5.396E+01	5.668E-02		
RUPT. STRAIN	1.698E-02	1.438E-01		

Figure 10.   Average Stress-Strain Curves of Transverse Compression Tests
of GY-70/934 (1 ksi = 0.145 MPa).

103

Figure 11a. Individual σ_2 vs ε_2 Curves for Biaxial Compression in 2-3 Plane for GY-70/934 (1 ksi = 0.145 MPa).

104

Figure 11b. Individual σ_3 vs ε_3 Curves for Biaxial Compression in 2-3 Plane for GY-70/934 (1 ksi = 0.145 MPa).

105

Office of Deputy Under Secretary of Defense
  for Research and Engineering (ET)
ATTN: Mr. J. Persh, Staff Specialist for Materials   1
      and Structures (Room 3D1089)
The Pentagon
Washington, DC 20301

Office of Deputy Chief of Research Development
  and Acquisition
ATTN: DAMA-CSS-D/Dr. J. I. Bryant (Room 3D424)   1
The Pentagon
Washington, DC 20310

Commander
U.S. Army Materiel Development and Readiness Command
ATTN: DRCLDC, Mr. R. J. Zentner   1
5001 Eisenhower Avenue
Alexandria, VA 22333

Director
Ballistic Missile Defense Systems Command
ATTN: BMDSC-TEN, Mr. N. J. Hurst   1
      BMDSC-H   1
      BMDSC-T   1
      BMDSC-AOLIB   1
P. O. Box 1500
Huntsville, AL 35807

Ballistic Missile Defense Program Office
ATTN: DACS-BMT   1
DARCOM Bldg., Seventh Floor
5001 Eisenhower Avenue
Alexandria, VA 22333

Director
Ballistic Missile Defense Advanced Technology Center
ATTN: ATC-M, Mr. M. Whitfield   1
      ATC-M, Dr. D. Harmon   1
      ATC-M, Mr. J. Papadopoulos   1
P. O. Box 1500
Huntsville, AL 35807

No. of Copies

Director
Defense Nuclear Agency
ATTN: SPAS, Mr. J. F. Moulton, Jr.   1
       SPAS, Mr. D. Kohler   1
Washington, DC 20305

Director
Army Ballistic Research Laboratories
ATTN: DRDAR-BLT, Dr. N. J. Huffington, Jr.   1
       DRDAR-BLT, Dr. T. W. Wright   1
       DRDAR-BLT, Dr. G. L. Moss   1
Aberdeen Proving Ground, MD 21005

Commander
Harry Diamond Laboratories
ATTN: DRXDO-NP, Dr. F. Wimenitz   1
2800 Powder Mill Road
Adelphi, MD 20783

Commander
U.S. Army Combat Development Command
Institute of Nuclear Studies
ATTN: Technical Library   1
Fort Bliss, Texas 79916

Commander
Air Force Materials Laboratory
Air Force Systems Command
ATTN: LNE/Dr. W. Kessler   1
       LNC/Dr. D. Schmidt   1
Wright-Patterson Air Force Base, Ohio 45433

Space and Missile Systems Organization
ATTN: RSSE/LTC J. McCormack   2
P. O. Box 92960
World Way Postal Center
Los Angeles, CA 90009

Commander
Naval Ordnance Systems Command
ATTN: ORD-03331, Mr. M. Kinna   1
Washington, DC 20360

Commander
Naval Surface Weapons Center
ATTN: Dr. C. Lyons   1
       Dr. W. Messick   1
Silver Springs, MD 20910

Lawrence Livermore Laboratory
ATTN: Dr. E. M. Wu
P. O. Box 808 (L-342)
Livermore, CA 94550

Los Alamos Scientific Laboratory
ATTN: GMX-6, Dr. J. W. Taylor
P. O. Box 1663
Los Alamos, NM 87544

Sandia Laboratories
ATTN: Dr. Frank P. Gerstle, Jr.   1
      Dr. L. D. Bertholf   1
      Dr. J. Lipkin   1
P. O. Box 5800
Albuquerque, NM 87115

Aerospace Corporation
ATTN: Dr. R. Cooper   1
      Dr. W. Barry   1
P. O. Box 92957
Los Angeles, CA 90009

AVCO Corporation
Government Products Group
ATTN: Dr. W. Reinecke   1
      Mr. P. Rolincik   1
201 Lowell Street
Wilmington, MA 01997

ETA Corporation
ATTN: Mr. D. L. Mykkanen   1
P. O. Box 6625
Orange, CA 92667

Effects Technology, Inc.
ATTN: Dr. R. Wengler   1
      Dr. R. Parisse   1
      Mr. J. Green   1
5383 Hollister Avenue
Santa Barbara, CA 93111

Fiber Materials, Inc.
ATTN: Mr. M. Subilia, Jr.   1
      Mr. L. Landers   1
      Mr. G. Williams   1
      Mr. P. Marchol   1
Biddeford Industrial Park
Biddeford, ME 04005

General Electric Company
Valley Forge Space Technology Center
ATTN: Mr. K. Hall
      Mr. J. Brazel
      Ms. B. McGuire
P. O. Box 8555
Philadelphia, PA 19101

General Dynamics Corporation
Convair Division
ATTN: Mr. J. Hertz
      Mr. H. McCutcheon, Jr.
5001 Kearny Villa Road
San Diego, CA 92138

General Dynamics Corporation
ATTN: Dr. D. J. Wilkins
Mail Zone 2884
P. O. Box 748
Fort Worth, Texas 76101

Kaman Sciences Corporation
ATTN: Mr. F. Shelton
P. O. Box 7463
Colorado Springs, CO 80933

Ktech
ATTN: Dr. D. Keller
911 Pennsylvania Avenue, N.E.
Albuquerque, NM 87110

Lockheed Missiles and Space Company
ATTN: Mr. D. Aspinwall
P. O. Box 504
Sunnyvale, CA 94088

Martin Marietta Aerospace
ATTN: Dr. M. Hendricks
      Mr. R. Hewitt
      Mr. Frank H. Koo
P. O. Box 5837
Orlando, Florida 32805

McDonnell Douglas Corporation
ATTN: Dr. L. Cohen
      Mr. H. Parachanian
5301 Bolsa Avenue
Huntington Beach, CA 92647

No. of Copies

Prototype Development Associates, Inc.
ATTN: Mr. J. Schultzler   1
        Mr. N. Harrington   1
1740 Garry Avenue, Suite 201
Santa Ana, CA 92705

R&D Associates
ATTN: Dr. A. Field   1
525 Wilshire Blvd.
Santa Monica, CA 90025

Radkowski Associates
ATTN: Dr. P. Radkowski   1
P. O. Box 5474
Riverside, CA 92507

Southwest Research Institute
ATTN: Mr. A. Wenzel   1
8500 Culebra Road
San Antonio, Texas 78206

Stanford Research Institute
ATTN: Dr. D. Curran   1
        Dr. L. Seaman   1
333 Ravenswood Avenue
Menlo Park, CA 90250

Terra Tek, Inc.
ATTN: Dr. A. H. Jones   1
420 Wakara Way
Salt Lake City, Utah 84108

TRW Systems Group
ATTN: Mr. D. Gamble   1
One Space Park
Redondo Beach, CA 90278

Lehigh University
Institute of Fracture and Solid Mechanics
ATTN: Dr. George C. Sih   1
Bldg. #19, Packard Lab.
Bethlehem, PA 18015

Stanford University
Department of Applied Mechanics
ATTN: Professor E. H. Lee   1
Stanford, CA 94305

University of Illinois at Chicago Circle
Department of Materials Engineering
ATTN: Professor R. L. Spilker
Chicago, Illinois 60680

Defense Documentation Center
Cameron Station, Bldg. 5
5010 Duke Station
Alexandria, VA 22314

Director
Army Materials & Mechanics Research Center
ATTN: DRXMR-H, Mr. J. F. Dignam
      DRXMR-H, Mr. L. Aronin
      DRXMR-H, Dr. S. C. Chou
      DRXMR-H, Dr. D. Dandekar
      DRXMR-AP
      DRXMR-PL
      DRXMR-PR
Watertown, MA 02172

Army Materials and Mechanics Research Center,
Watertown, Massachusetts 02172
STRESS ANALYSIS AND STRENGTH
CHARACTERIZATION OF THICK COMPOSITE
LAMINATES
Edward M. Wu, Ging Hin Lo, and
Richard M. Christensen,
Materials Research Laboratory,
Washington University 63130
St. Louis, Missouri 63130
Technical Report AMMRC TR 79-29, May 1979, 105 pp -
illus-tables, Contract DAAG46-75-C-0096
D/A Project 1J663J00482J5, AMCMS Code 633J04.21500.03
Final Report, June 30, 1975 to June 25, 1976

AD

UNCLASSIFIED
UNLIMITED DISTRIBUTION

Key Words

Composites   Stresses
Lamina   Mechanical tests
Plate Theory   Elasticity
                Fracture & Strength

The objectives of this research program were to develop a theoretical stress analysis and strength characterization for thick composite laminates and to check the theory against experimental results. A new high-order theory of plate deformation for both homogeneous and laminated plates was developed, which accounts for the effects of transverse shear deformation, transverse normal strain, and a non-linear distribution of the in-place displacement with respect to the thickness coordinate. The theory provides close estimation of 3-dimensional stress components from a 2-dimensional analysis. The effects of 3-dimensional state of stress on the strength of thick laminates were analyzed with a 3-dimensional, tensor polynomial failure criterion, and experimental evaluations of the approach were made.

Army Materials and Mechanics Research Center,
Watertown, Massachusetts 02172
STRESS ANALYSIS AND STRENGTH
CHARACTERIZATION OF THICK COMPOSITE
LAMINATES
Edward M. Wu, King Hin Lo, and
Richard M. Christensen,
Materials Research Laboratory,
Washington University,
St. Louis, Missouri 63130

Technical Report AMMRC TR 79-29, May 1979, 105 pp -
illus-tables, Contract DAAG46-75-C-0056
D/A Project B163390D215, AMCMS Code 6)3)04.21500.0)
Final Report, June 30, 1975 to June 29, 1976

Key Words

Composites	Stresses
Lamina	Mechanical tests
Plate Theory	Elasticity
	Fracture & Strength

The objectives of this research program were to develop a theoretical stress analysis and
strength characterization for thick composite laminates and to check the theory against
experimental results. A new high-order theory of plate deformation for both homogeneous
and laminated plates was developed, which accounts for the effects of transverse shear
deformation, transverse normal strain, and a non-linear distribution of the in-place
displacements with respect to the thickness coordinates. The theory provides close
estimation of 3-dimensional stress components from a 2-dimensional analysis. The effects
of a 3-dimensional state of stress on the strength of thick laminates were analyzed with
a 3-dimensional, tensor polynomial failure criterion, and experimental evaluations of the
approach were made.